ANALYSIS OF INDIUM AND CADMIUM ACTIVATED TO

METASTABLE STATES WITH COBALT-60 GAMMA-RAYS

by

Satoshi Minakuchi

A Thesis Submitted to the

Graduate Faculty in Partial Fulfillment of

The Requirements for the Degree of

MASTER OF SCIENCE

Major Subject: Nuclear Engineering

Iowa State University
Ames, Iowa

1970

TABLE OF CONTENTS

iii

LIST OF FIGURES

LIST OF TABLES

I. INTRODUCTION

Some nuclides can be activated to metastable states by gamma-rays with sufficiently high energy, and then the activated nuclei may produce gamma-rays from isomeric transitions. If the decay gamma-rays are detected with a suitable nuclear radiation measurement method, the sample nuclides can be analyzed qualitatively and quantitatively. This is a basic concept of gamma activation analysis.

Approximately 250 nuclear isomers are presently known with half lives between 10^{-10} sec. and several years (1), but not all of these isomers qualify for gamma activation analysis because there is a limitation of detectable activity. Table 1 is a list of isomers which have possibilities of gamma activation. Lukens et al. (2) discussed the possibility of activation of isomers with bremsstrahlung produced by electrons accelerated in a Van de Graaf generator. Desoete, et al. (1) discussed reaction thresholds, reaction cross section, and the procedure of photon production. The subdivision of activation analysis which is called photoactivation analysis or gamma activation analysis employs the (γ, γ') reaction, and can be classified also as a method of activation to excited levels, e.g., by utilization of bremsstrahlung or artificial radioisotopes.

The first trial of gamma-activation by Co-60 gamma-rays

was performed by Harbottle (3) in 1954. He used Co-60 sources
with activities from 170 curies to 1800 curies and a 1300-
curie Ta-182 source to investigate the ratio of dose rate of
gamma-ray source to intensity of activity of indium and
cadmium activated by gamma-rays.

After Harbottle, Ikeda, et al. (4-12), developed both
experimental and theoretical work on (γ,γ') activation
analysis. They discussed gamma-ray activation of indium
(4,5), rhodium (4), and silver (8), activation cross-
sections for In-115(γ,γ')In-115m (6,7), Cd-111(γ,γ')Cd-111m
(9), Rh-103(γ,γ')Rh-103m (11), and Sr-87(γ,γ')Sr-87m (12),
and photon dosimetry as an application of gamma activation
(10). Yoshihara (13-17) discussed the theoretical background
of activation cross section for (γ,γ') reaction (13-15),
indium dosimetry (16), and practical gamma activation
analysis of indium in a compound metal such as indium and
tin (17). His study of indium dosimetry is a very practical
and useful application of gamma-ray activation analysis.

More recently, Veres (18), Veres and Pavlicsek (19, 20),
and Law and Iddings (21) contributed articles in this field.
They investigated activation cross-section for In-115(γ,γ')
In-115m reaction, but they did not agree on a common value.
It is difficult to determine the gamma activation cross-
section when there is no method of obtaining a highly accurate
value of gamma flux in a very high dose rate field.

Table 1. Nuclear isomers available for gamma activation analysis (22)

Element	Abundance	Half life	Energy of γ-ray (keV)[a]	Reference
Se-77m	7.58%	17.5s	161(50%)	2,20
Br-79m	50.5	4.8s	210	20
Kr-83m	11.55	1.86h	9.3,32.5	2
Sr-87m	7.02	2.83h	388(80%)	2,12,15,21
Y-89m	100	16s	910(99%)	2
Rh-103m	100	57m		2,4,11,15,21
Ag-107m	51.35	44.3s	94(50%)	8,15,20
Ag-109m	48.65	40s	88(5%)	2,8,15,20
Cd-111m	12.75	48.6m	150(30%),246(94%)	2,3,9,15,18,20,21
In-113m	4.23	100m	393(64%)	19,21
In-115m	95.7	4.5h	335(50%)	2-7,15-18,20,21
Sn-117m	7.57	14.0d	158(87%)	2
Xe-129m	26.44	8.0d	40(9%),196(6%)	
Xe-131m	21.18	11.8d	164(2%)	
Ba-135m	6.6	28.7h	268(16%)	21
Ba-137m	11.3	2.55m	662(89%)	2
Er-167m	22.94	2.3s	208(43%)	
Yb-176m	12.7	11s	104(65%),228(13%)	
Lu-176m	2.6	3.69h	88(10%)	2,15,21
Hf-179m	13.7	18.6s	217(94%)	2

[a]The percentages in this column are probabilities of gamma-ray emission.

Table 1 (Continued)

Element	Abundance	Half life	Energy of γ-ray (keV)[a]	Reference
Hf-180m	35.22	5.5h	1142(m.s.level)	21
Ta-180m	0.012	8.1h	93(4%),103(0.6%)	21
W-183m	14.4	5.3s	309(m.s.level)	
Os-189m	16.1	5.7h	30.8(m.s.level)	21
Os-190m	26.4	9.9m	1706(m.s.level)	21
Ir-191m	38.5	4.9s	129(25%)	2
Pt-195m	33.8	4.1d	99(11%),129(1%)	2
Au-197m	100	7.2s	130(8%),279(75%)	2
Hg-199m	16.84	43m	158(53%),375(15%)	2,21
Pb-204m	1.4	67m	375(93%),900(189% doublet)	21

The experiments of Yoshihara, Veres, and Law were closely related to this research. It is helpful to tabulate and compare the results of their work in Table 2.

Compared to neutron activation analysis, gamma activation analysis had disadvantages and difficulties as much as it has advantages and simplicity. One of the difficulties of gamma activation analysis is that of radiation measurements, because the activity is generally very low and the energy of the isomeric transition is very small. Therefore, the factors of background and statistical error become important, and this kind of problem should be solved with shielding techniques

Table 2. Summary of results from Yoshihara, Veres, and Law for gamma activation of In-115 with Co-60 source (4-21)

	Yoshihara	Veres	Law
Intensity of Co-60 source (curies)	10,000	2,900	5,000
Equipment for measurement	1.75 in. x 2 in. NaI, spectrometer	1.5 in. x 1.75 in. NaI, single ch. PHA	3 in. x 3 in. NaI, 400 ch. PHA
Specific count rate (cpm/g In)	1283	277	451
Cross-section (cm^2)	2.9×10^{-32}	4.9×10^{-32}	2.0×10^{-32}
Mass of target (g)	~2	~20	0.5 to 10
Minimum detectable amount (g)	–	–	0.025
Dose rate, or gamma flux	2×10^6 (r/hr)	2.2×10^{11} (γ/cm^2sec)	1.4×10^4 (rad/min)

and careful statistical analysis of data. Watt and Ramsden (23) contributed to the method of analysis of very low counting rate data. They discussed sources of background, attainment of low background, and counting parameters techniques. Although gamma activation analysis has difficulties as mentioned before, the simplicity of its activation, instrumentation, and data analysis is the most remarkable advantage.

There are various types of activation analysis which utilize metastable states, and each may be recognized by the radiation particles which cause activation, e.g., neutrons, electrons, and protons, but gamma activation analysis is limited to gamma-rays, only. Gamma activation analysis was classified by method of activation to excited energy levels, and furthermore it can be classified by the type of emitted radiation. Baker discussed the types of gamma activation analysis in his article (24). A summary of the types of gamma activation and their explanations follows:

(γ, γ) reaction   This type of reaction is called the Mössbauer effect. Gamma-rays with a few hundred keV are emitted by excited states, and sometimes they can be re-absorbed by other nuclei of the same isotope (25). Unfortunately, there is no analytical method based on this effect to date.

(γ,γ') reaction   When a certain stable nuclide inter-
acts with a gamma-ray of sufficiently high energy, the nuclide
is activated from its ground state to a higher level which
instantly decays to the metastable state. When the nucleus
decays by isomeric transition, the excess energy may be
emitted as a photon, and the isomer decays with a measurable
half-life. By detecting the emitted photons, the sample can
be qualitatively and quantitatively described. This type of
gamma activation was employed in this investigation.

(γ,n) reaction   If the sample could be irradiated with
gamma-rays of higher energy (10-25 MeV) than that in the case
of (γ,γ') reaction, this kind of reaction may occur. Most
of the gamma-induced analytical work utilizes this reaction.
If the source gamma-rays have much higher energy than that
for the case of (γ,γ') reaction, ($\gamma,2n$), (γ,p), (γ,pn), or
($\gamma,\alpha n$) reactions may occur. Engelmann (26) tried (γ,n) and
(γ,p) reactions with the use of bremsstrahlung sources.
Actual examples of the analytical possibilities are described
in his article. In particular, he determined very small
quantities ($<10^{-6}$) of C, N, O, and F.

This investigation has been aimed at two objectives: to
investigate the feasibility of (γ,γ') activation analysis
as a tool for analysis of indium and cadmium, and to predict
sensitivity and precision of mass determinations for specific
experimental conditions.

II. THEORY

The process of activation analysis can be separated in three steps, namely, (i) irradiation of sample, (ii) measurements of sample activity, and (iii) data analysis based on statistical procedures. It is also necessary to make clear the mathematical formulations for each step and terminology which are employed here.

A. Irradiation

Figure 1 is a schematic of activity as a function of time for a single radioisotope. Between points S and T, the sample is exposed to a constant intensity field of gamma-rays. The activation curve between S and T is increasing with time,

$$A(t) = N_T \sigma \phi (1 - e^{-\lambda t}),$$ (1)

where A is activity and is a function of time, σ is an activation cross-section, ϕ is the gamma flux, and N_T is the total number of nuclei of the sample which is given by

$$N_T = \frac{Wg}{M} N_O,$$ (2)

where W is the mass of the sample g is the abundance of the isotope, M is its atomic weight and N_O is Avogadro's number. If the irradiation time, t_i, is long enough (about 10 times
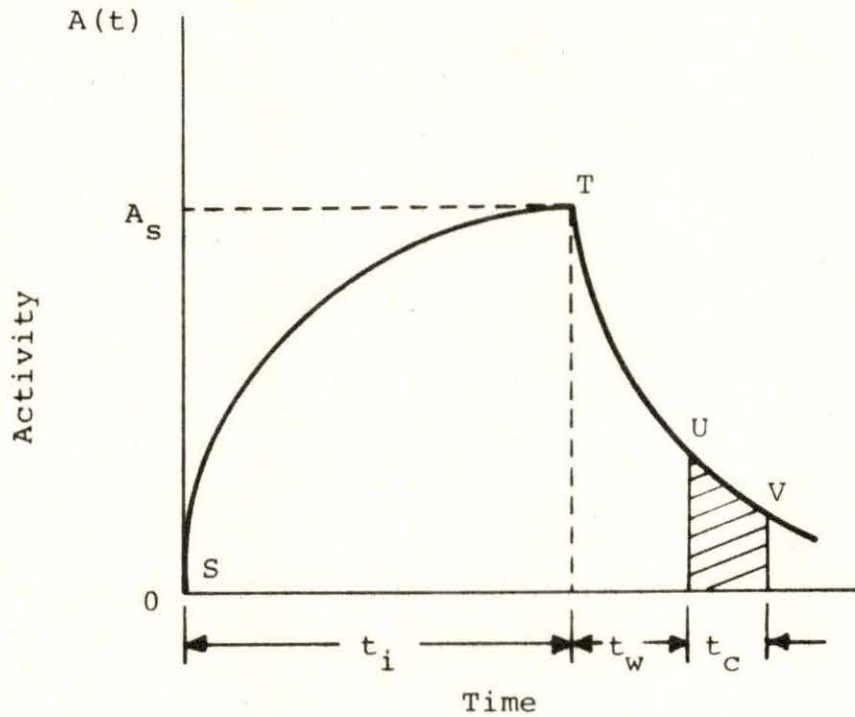
Figure 1. Activity as a function of time (The irradiation
           starts at S and ends at T for irradiation time t_i.
           The radiation measurement starts at U and stops
           at V.   The terms t_w and t_c mean waiting time and
           counting time, respectively)

its half life), the exponential term in Equation 1 is negligible, and Equation 1 is changed to

$$A_s = N_T \sigma \phi, \tag{3}$$

where A_s is distinguished from A, because A_s is not a function of time, and is defined as a saturated activity.

The gamma-ray flux is a complicated function of position and energy within the irradiation facility. When the intensity of gamma rays in a radiation field is discussed the term dose rate D is generally used, and its unit is usually rad/min. The relation between D and gamma flux ϕ, as developed by Glasstone and Sesonske (27, p. 427), is given by

$$D = \frac{\phi E_\gamma \mu_e}{6.2 \times 10^7}, \tag{4}$$

where

D is the dose rate in rad/min.,

E_γ is the photon energy in MeV, and

μ_e is the energy absorption coefficient in air, cm^2/gm.

When gamma-rays produced from Co-60 are considered, the energy is taken as the mean value of both gamma-rays, namely,

$$E_\gamma = 1.25 \text{ MeV} .$$

The energy absorption coefficient for air can be obtained

from nuclear data tables (28), where the value is given

as

$$\mu_e = 0.0268 \text{ cm}^2/\text{gm for } 1.25 \text{ MeV-}\gamma \quad .$$

These values, when substituted into Equation 4, give the

gamma flux,

$$\phi(\text{photons/cm}^2 \text{ min}) = (1.85 \times 10^9) \text{ D(rad/min)} \quad . \quad (5)$$

Theoretical consideration of activation cross-section

for (γ,γ') reaction is very complicated. Yoshihara made a

comprehensive theoretical study of the cross-section (13,14).

The first part of his Japanese language article (13) is

briefly translated:

The (γ,γ') reaction is an excitation reaction of
the nuclide by resonance absorption of a gamma-ray with
a certain energy. Since the nuclear spin of a nuclide
in a metastable state is greatly different from that
of a stable-state nuclide, the transition from the
metastable to the stable state is highly forbidden.
Therefore, the nuclide in the metastable state decays
with a measurable half-life. Gamma-rays from artificial
radioactive isotopes have very narrow energy width,
and in general, their energies do not overlap the
resonance level corresponding to the (γ,γ') reaction.
Some part of the energy spectrum which is distributed
by Compton scattering would contribute to the (γ,γ')
reaction. One of the necessary conditions on gamma-
rays from the radioactive isotope is that their energy
is larger than or equal to the lowest excitation
energy level of the (γ,γ') reaction.
In order to discuss the (γ,γ') reaction with gamma-
rays produced from an artificial radioisotope, one must
be concerned with how the Compton-scattered gamma-rays,
with energy equal to the excitation level which
contribute to (γ,γ') reaction in a target material, will
be produced.

Study of the activation cross-section of the (γ, γ') reaction is important for gamma activation analysis, but it is beyond the scope of this investigation.

B. Measurement

At the point T in Figure 1, the sample with an activity of A_s is taken from the irradiation facility (Co-60 source), and the activity decays as

$$A(t) = A_s e^{-\lambda t}, \tag{6}$$

where t is the time starting at the end of irradiation. During a certain waiting time, t_w, the sample is set up in a suitable radiation measurement system. The counting period starts at the point U and stops at V. Accumulated value during a counting time t_c corresponds to the number of gamma-rays detected as a result of decay, namely, the area under the decay curve in the region of UV in Figure 1. Let A_T be defined as the total activity during the counting time t_c, and given by

$$A_T = A_s \int_{t_w}^{t_w + t_c} e^{-\lambda t} dt = A_s \frac{1}{\lambda} e^{-\lambda t_w} (1 - e^{-\lambda t_c}). \tag{7}$$

With this equation, the total activity A_T is equivalent to an area designated by the oblique lines in Figure 1.

An observed value obtained with a suitable radiation

measurement system is not equal to A_T, and some modification
from A_T has to be considered. Overman and Clark (29)
developed the modification factors for general cases in
Section 7-2. Modification factors for special cases have
to be considered here, which are for gamma-ray measurement
with a multichannel analyzer.

Let C_T be defined as a total observed count in the
photopeak during the counting time t_c, and then the relation-
ship between C_T and A_T given in Equation 7 can be written
as,

$$C_T = A_T \cdot G \cdot f \cdot P(IT) \cdot \frac{1}{\alpha+1} \cdot s \cdot p \quad , \tag{8}$$

where

> G is a factor depending on the geometrical condition
> between the sample and the detector,

> f is an overall detector efficiency for the particular
> radiation,

> P(IT) is a probability that the decay is an isomeric
> transition,

> α is the internal conversion coefficient, and
> therefore, $1/(\alpha+1)$ is the probability that the
> I.T. produces a gamma rather than an internal con-
> version electron plus x-rays,

> s is a self absorption factor in the sample material,

> p is a ratio of photo peak to total counts in the
> gamma-ray spectrum.

If R is the counting rate at the end of the irradiation, and
since C_T is a value actually observed, the next equation will
be useful to calculate a value of R.

$$R = \frac{\lambda C_T}{e^{-\lambda t_w}(1-e^{-\lambda t_c})} \qquad . \qquad\qquad (9)$$

When various samples are counted separately and compared, their counting rates are derived from the measured counts C_T through Equation 9. If the irradiation time is long enough (about 10 times the half-life), irradiation time correction is not necessary, and only the waiting and counting time corrections should be taken into consideration.

C. Data Analysis

A given sample was irradiated, and its activity was measured after removal from the gamma field. The readout data from a multichannel analyzer were printed separately for each channel corresponding to a given gamma-ray energy. The shape of the observed gamma-ray spectra of indium is shown in Figure 9. The total spectrum is usually distorted at the low-energy end by electronic noise and uncertainty in multichannel analyzer address assignments in the first few channels. These experimental difficulties are avoided, when the photopeak is investigated. The ratio of area under the photopeak curve to that of the whole spectrum (i.e. the peak to total ratio, p) depends upon the energy of gamma-rays and the geometric condition of the counting system. Therefore, if the counts under the photopeak curve could be obtained

accurately, the total count could be determined with the peak-to-total ratio for a particular energy of gamma-rays and the geometric condition. Experimental peak-to-total ratios for 3 in. x 3 in. NaI detectors were investigated by Heath (30). The peak-to-total ratio versus gamma-ray energy on a logarithmic graph appears in his report.

In practice, a photopeak curve can be assumed to follow a Gaussian (normal) distribution function (30). The equation for the Gaussian distribution is given in any general statistics text (e.g., 31, 32) or in the statistics section of many nuclear radiation texts (e.g., 33, 34). A general Gaussian distribution function is given by

$$f(x) = \frac{1}{\sqrt{2\pi}\sigma} \exp \left[- \frac{(x_o - x)^2}{2\sigma^2}\right] \quad , \tag{10}$$

where $f(x)$ is the normalized Gaussian distribution function of the variable x, x_o is the mean value, and σ is the standard deviation. This equation can not be directly used to represent the photopeak, because the photopeak is not normalized.

A modified equation is necessary, such as,

$$G(x) = A_{max} \exp[-B(x_o - x)^2], \tag{11}$$

where $G(x)$ is the count in channel x in a gamma-ray spectrum, A_{max} is the count at $x = x_o$, and B is equal to $1/(2\sigma^2)$ in

Equation 10. Procedures used to find the constants, A_{max}, B
and x_O will be discussed later. The area under the Gaussian
curve expressed with Equation 11 can be simply calculated by
the following method:

Integration of Equation 11 over all values of x gives
the area under the photopeak curve fitted with the Gaussian
function,

$$\text{Area} = \int_{-\infty}^{\infty} G(x)\,dx = A_{max}\int_{-\infty}^{\infty} \exp[-B(x_O-x)^2]\,dx \qquad (12)$$

The integration of the exponential is calculated from the
definition of the normalized Gaussian distribution function
expressed by Equation 10, namely,

$$\int_{-\infty}^{\infty} f(x)\,dx = 1, \qquad (13)$$

then,

$$\int_{-\infty}^{\infty} \exp\left[-\frac{(x_O-x)^2}{2\sigma^2}\right]dx = \sqrt{2\pi}\sigma . \qquad (14)$$

Since $B = 1/(2\sigma^2)$, Equation 12 becomes

$$\text{Area} = \sqrt{2\pi}\sigma A_{max}, \qquad (15)$$

Let C_{TP} be a total count under the fitted-photopeak
curve, i.e., C_{TP} = Area. Equation 15 rewritten with the
constant B gives

$$C_{TP} = \sqrt{\frac{\pi}{B}} \, A_{max} \; . \tag{16}$$

From this equation, by knowing the constants A_{max} and B, the total counts under the fitted-photopeak curve can be calculated.

The method of fitting the Gaussian curve to the data points of the photopeak should be discussed next. The method of least squares is used frequently in drawing a curve on data points and is discussed in many general books in the field of statistics and scientific experiments (35). One of the practical methods was discussed by Bevington (32). He used the following function for a Gaussian peak plus a quadratic background:

$$y(x) = a_1 \exp\left[-\frac{1}{2}\left(\frac{x-a_2}{a_3}\right)^2\right] + a_4 + a_5 x + a_6 x^2 \; , \tag{17}$$

where a_i (i = 1,2,...,6) are parameters. He also discussed the method of non-linear least squares and presented some computer programs. One of them was tried, and the results and details are discussed in Appendix D.

Heath (30) used another function to fit photopeak data. If his function is written with his own terms, it is given by:

$$y(x) = y_o \exp\left[-(x-x_o)^2/b_o\right]\left[1 + \alpha_1 (x-x_o)^4 + \alpha_2 (x-x_o)^{12}\right] \; , \tag{18}$$

where the powers 4 and 12 were chosen to give the best fit, and x_o, y_o, b_o, α_1, and α_2 are the parameters determined in the fit. A non-linear least-squares fitting program was prepared to calculate the above five parameters.

In this investigation, a completely different procedure was employed as follows:

(1) The region of data population which may contribute to the calculation is determined.

(2) In the region which is selected in step (1), a certain Gaussian fitting function is found by employing the method of least squares.

(3) For the final fitted-Gaussian curve, goodness of fit is confirmed with the χ^2-test.

An accurate result can not be expected if all data near the photopeak are used to fit a Gaussian curve, because each datum can not be statistically weighted at the same level. Statistical values of the data points around the top and the tail of the photopeak curve are very different (c.f. Figure C-2), because those around the tail have high probability of containing some other components (e.g. another photopeak). Therefore, it is necessary to select a certain region of data.

Figure 2 shows a truncation method using the reduced χ^2 value for finding the region. At first, one boundary of the region is fixed, and then the other boundary is moved

along the side of the photopeak. Then each value of the
reduced χ^2, (which will be defined later) is plotted versus
channel number as in Figure 2. The channel number indicating
the minimum reduced χ^2 is a limit on that side of the
region. The limit of the other side of the peak can be
obtained analogously. In the case of Figure 2, the selected
region is that between channels -15 and +11.

It is very time consuming to use the above procedure of
selecting the region of data for least squares fitting.
Therefore, a simple method was mainly employed for this in-
vestigation. From examination of data using the "student-
t" tail test, the region can be determined. In section
3.6 of (31), the method of this test was discussed in
detail.

Let $z(x_i)$ be the value of "student-t" for the channel
number x_i and be defined by

$$z(x_i) = \frac{|C(x_i)-G(x_i)|}{\sigma(x_i)} \quad , \tag{19}$$

where $\sigma(x_i)$ is the standard deviation of the experimental
value $C(x_i)$ calculated from the original total count
$C_{sb}(x_i)$ for counting time t_c and the background count
$C_b(x_i)$ for counting time t_b. It is given by

$$\sigma(x_i) = [C_{sb}(x_i) + (\frac{t_c}{t_w})^2 C_b(x_i)]^{\frac{1}{2}} \quad . \tag{20}$$

Figure 2. Determination of fitting region using minimum reduced χ^2
(Data corresponds to No. 12 of indium)

Figure 2. Determination of fitting region using minimum reduced χ^2
(Data corresponds to No. 12 of indium)
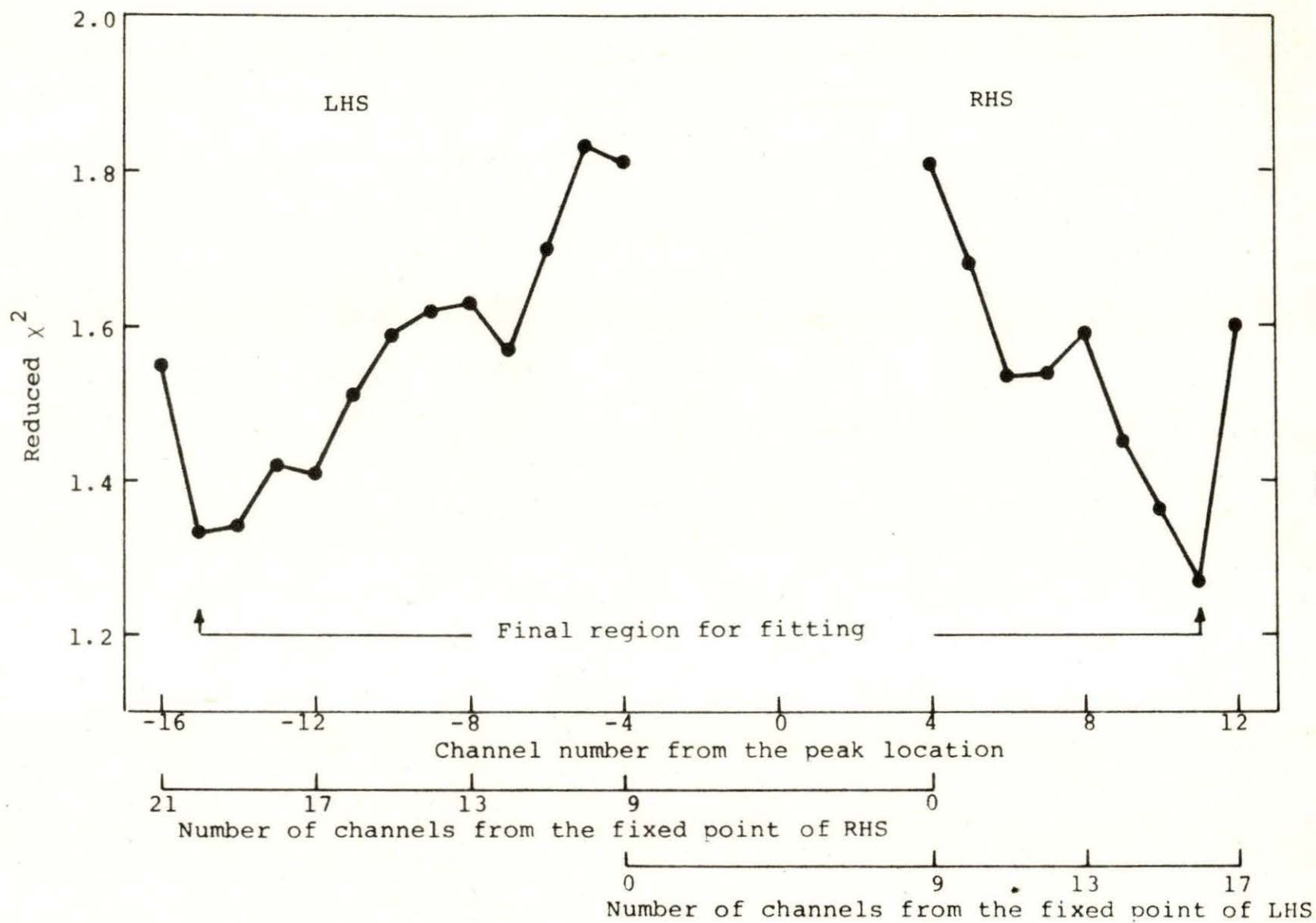
The relationship among these three counting values is

$$C(x_i) = C_{sb}(x_i) - (\frac{t_c}{t_b})C_b(x_i) \ . \tag{21}$$

From the distribution of $z(x_i)$, the region boundaries can be determined. The value of $z(x_i)$ is consistently small if the individual net count indicated by $C(x_i)$ is not greatly different from the expected value $G(x_i)$. If the datum point deviates strongly from $G(x_i)$ it is assumed to be out of the region, and the value of $z(x_i)$ increases conspicuously.

The second step of data analysis is to fit the Gaussian function to the data. To fit the photopeak curve data, a one-dimensional least squares method can be used, because one of the dimensions of the data is the channel number which can be fixed.

Let "Sum" be a summation of square values of the differences between the observed values $C(x_i)$ and the expected values $G(x_i)$ such as

$$Sum = \sum_{i=1}^{n} [C(x_i)-G(x_i)]^2 \ , \tag{22}$$

where i is the index of the channel number, and the maximum index n is selected in step (1). The final Gaussian function, which is defined by Equation 12, is obtained by minimizing the value of "Sum".

As the third step, χ^2, reduced χ^2, and degrees of freedom should be defined next.

The χ^2-test is often used in statistics, and discussed in many references on statistical methods. Steel and Torrie (31) gave the test criterion with a simple equation in their Chapter 19, that is

$$\chi^2 = \Sigma \frac{(\text{observed} - \text{expected})^2}{\text{expected}} \qquad (23)$$

This form of chi-square is valid for Poisson distributions since it is assumed that the variance in the definition of χ^2 is replaced by the mean (which is the expected) value. Bevington (32, p. 85) described applications of χ^2-test, and it is valuable to repeat his description.

> In order to test the goodness of fit of observed frequencies to the assumed probability distribution, we must know how χ^2 is distributed; i.e., we need to know the probability of observing our calculated value of χ^2 from a random sample of data. If such a value is highly probable, then we can have confidence in our assumed distribution and vice versa.

If Equation 22 is applied to the Gaussian curve fitting, $C(x_i)$ would be the observed value, and $G(x_i)$ would be the expected value. The summation of the χ^2 equation is over the region which was selected in step (i). The χ^2 equation can be rewritten with $C(x_i)$ and $G(x_i)$ and given by

$$\chi^2 = \sum_{i=1}^{n} \frac{[C(x_i) - G(x_i)]^2}{G(x_i)} . \qquad (24)$$

Reduced χ^2 can be calculated by dividing χ^2 by the value of "degrees of freedom" ν, namely χ^2/ν. This statistic is used when some values of χ^2 with different degrees of freedom are to be compared with each other. Bevington (32, p. 89) defined ν as "the number of data points n minus number of parameters of the distribution determined from these data points."

In the case of Gaussian curve fitting, since B and x_o are used in the calculation of the Gaussian parameters, then the number of parameters is two. Thus the degrees of freedom is given by

$$\nu = n - 2 , \tag{25}$$

where n is defined as the number of channels which contribute to the Gaussian curve fitting.

III. IRRADIATION FACILITY

The source of gammas used to activate the indium and cadmium samples was the artificial radioisotope cobalt-60. Since the probabiltiy of producing an isomer by gamma bombardment is extremely small, a very high dose-rate irradiation facility is required. Based on previous experiments (c.f. Table 2), the necessary Co-60 activity to achieve a reasonable sample activity could be estimated.

The Nuclear Engineering Gamma Irradiator has been described by other investigators (36, 37), but some details important to this experiment are repeated here. In addition, the information in this section would be valuable in the planning and design of a high dose-rate facility. The six sources used in the facility shown in Figure 3 contain approximately 5000 curies total activity. Characteristics of these sources are listed in Table 3. The outer twelve capsule holders were vacant during the experiment. A cross sectional view of a single source capsule is presented in Figure 4. All six of the source clusters move in unison on an arc toward the sample container (in the center of the drawing) from the storage position at the other extreme of travel. The sources were positioned by adjusting a calibrated hand-wheel. Since maximum dose rate was desired during the experiment, the source clusters were positioned so that they

Table 3. Characteristics of Co-60 source in the irradiation
facility

U.S.A.E.C. Licence number	14-00019-08
Made by	U.S. Nuclear Corporation, Burbank, California
Chemical form and method of deposition	solid metal, gold or nickel plated
Source capsule	Type 365, Ref. USN Drawing B-0094
Materials of construction	Type 321 stainless steel (except external magnetic end piece, 416 stainless steel)
Window or minimum wall	doubly encapsulated, minimum total wall 0.040 inch
Overall dimensions	1/2 in. dia. x 5 3/4 in. long
Method of sealing	Heliarc weld

touched the sample container.

The sample container was made of brass and was positioned
along a line perpendicular to the plane of the drawing in
Figure 3. To achieve maximum exposure, the sample
holder was adjusted until the sample was at the mid-elevation
of the cluster of sources. At this position, the dose rate
(Fricke method) was approximately 10^4 rad/min.

The biological shield degrades the energy spectrum of
the gamma rays primarily through Compton scattering, and hence,
aids in providing moderated gammas for the resonance
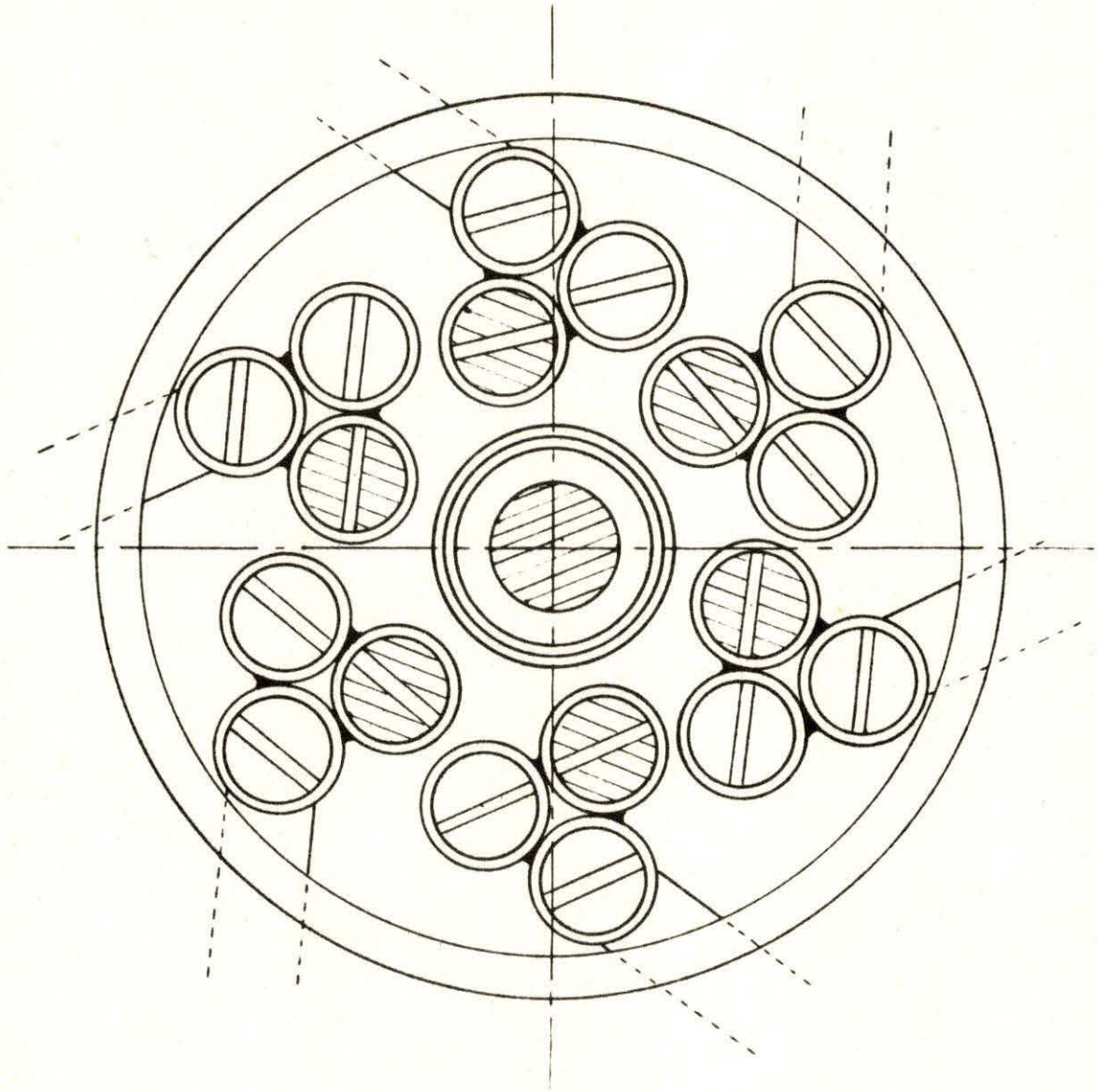excitation reaction. A thorough study of the exact role of

Figure 3. Horizontal cross-section of Co-60 source
clusters (Inner six capsules contain
Co-60 isotope, but the others are empty.
The shaded circle at the center is the sample
foil location, (1/2 in. dia.))

Figure 4. Dimensions of the Type-365 source capsule

	Material	Description
1.	321 St.St.	Outer capsule 0.50 in. od. - 0.46 in. id.
2.	321 St.St.	Inner capsule 0.45 in. od. - 0.41 in. id.
3.	321 St.St.	Outer plug
4.	321 St.St.	Inner plug
5.	Co-60	Radioisotope
6.	416 St.St.	Magnetic end piece
7.	St.St.	1/16 in. Roll pin

29

5 3/4"

5"

3/8"

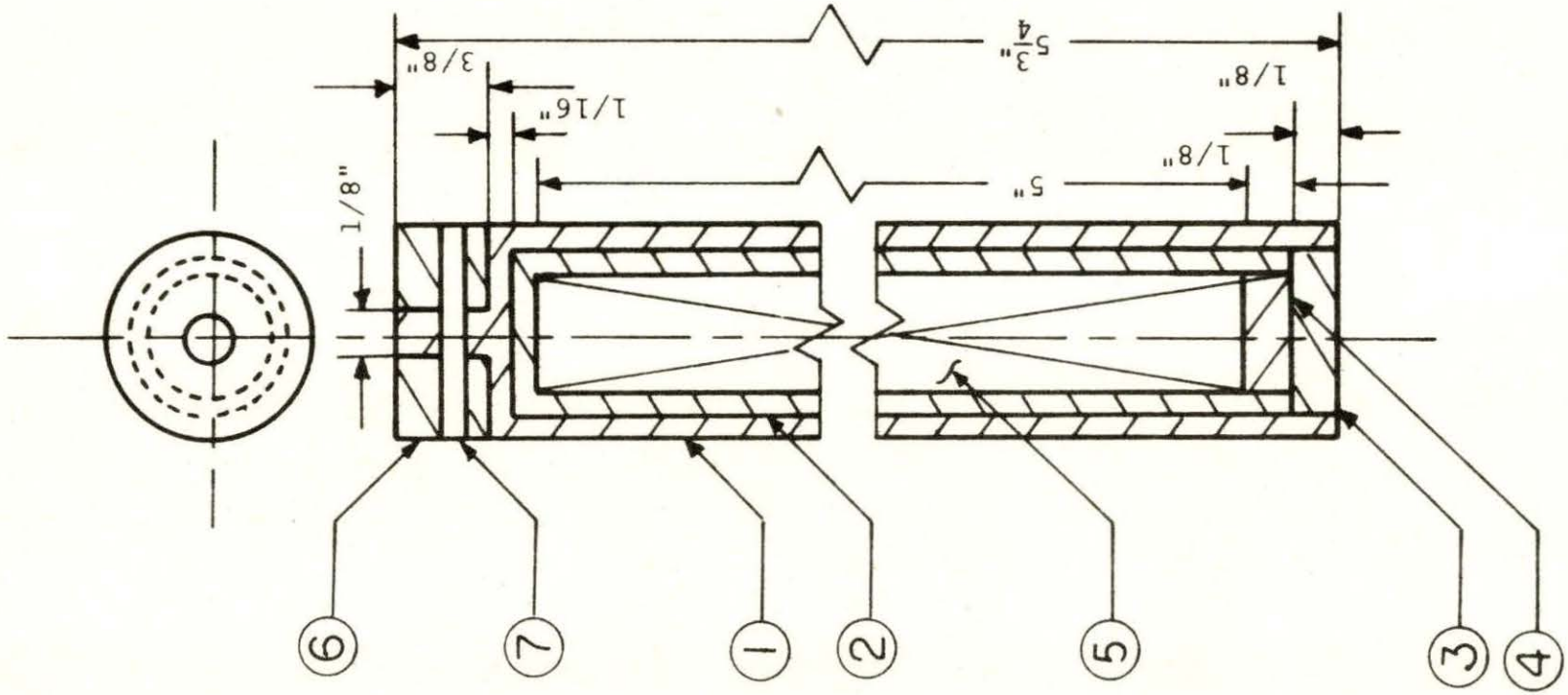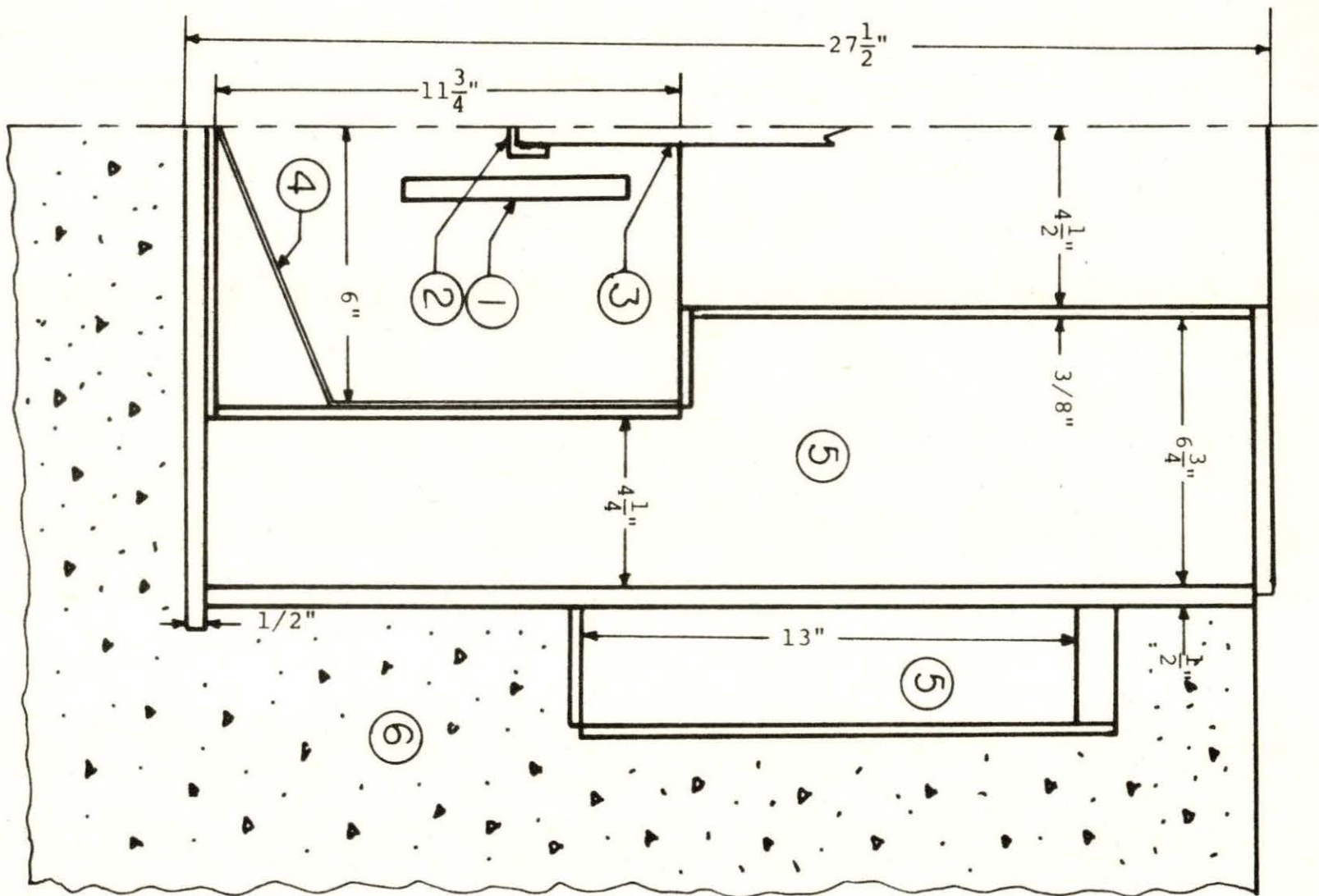1/16"

1/8"

1/8"

1/8"

6 7 1 2 5 3 4

Figure 5.   Vertical cross-section of the Co-60 irradiator

1.   0.5 in. diameter disk foils of sample
2.   Co-60 source capsule (c.f. Figure 3)
3.   Brass tube sample holder
4.   18 G.A. stainless steel
5.   Lead fill
6.   Concrete

the shield in modifying the gamma energy flux is beyond the
scope of this investigation, however, by noting the geometric
relationships of sample, source, and shield, recognition is
given to the importance of the shield configuration. The
source clusters are centrally located within a cylindrical
cavity approximately 12 inches in diameter and 11-3/4
inches in height. The diametral cavity wall is lined with
lead 4-1/4 inches thick. The entire shield is imbedded in
concrete so that the top surface is at floor level. The top
of the cavity is provided with a 4-1/2 inch radius passage-
way for the sample container and following shield plug.

IV. RADIATION MEASUREMENT EQUIPMENT

The combination of low activity, low energy gamma-rays (less than 0.5 Mev), and relatively short half-life of the nuclear isomers requires extra care in assemblying a measurement system. Also, background activity can no longer be treated as a negligible factor.

Counting data derived from measurements of sample activity will have acceptable precision and accuracy only if the effects of background are carefully considered. Low energy gamma-ray measurements are further complicated by an increase in background detection rate as the energy decreases. This does not imply an increase in activity at lower energies, but rather an effect observed as a result of instrumental response to the background activity.

Origins of background activity, attainment of low background counting rate, and counting techniques in background radiation environments were discussed by Watt and Ramsden (23). Fundamental sources of background observations in a counting system are:

(1) cosmic rays which interact with the detector either directly or indirectly,

(2) local radioactivity in materials close to the detector or in it,

(3) extraneous pulses from electronic components, and

(4) obvious sources of activity, such as, radio-
isotopes, nuclear reactors, etc.

Some of these sources can be eliminated while the effects of
others can only be minimized. A shield of high density
material, e.g., lead, is commonly used to reduce background.

Heath (30) developed a standard shield (32 in. cube
inside) for NaI scintillation spectrometry which reduced the
backscatter radiation to a minimal level. His data show
that the photopeak region of the gamma spectrum is not
noticeably affected by shields as small as 6 in. square by
18 in. high in internal dimensions. The shield used in
this experiment is shown in Figure 6 in cross-sectional view.
The internal cavity, a one-foot cube, is lined with cadmium
and copper similar to Heath's shield.

The samples under study were disks of various thickness,
but all were one-half inch in diameter. To be reasonably
sure of reproducible sample-detector geometry, a sample
holder pictured in Figure 7 was constructed of plexiglass
and positioned so that the sample to crystal distance was 1.1
cm. X-ray films of the detector provided access to the
crystal-to-cover distance.

The detection system shown in Figure 8 was used in
this investigation. A detailed listing of equipment appears
in Table 4. One variation of the basic system was considered
and tested. Two 3 in. x 3 in. NaI detectors were employed

Figure 6. Vertical cross-section of the detector shield

        1. Plug for sample access
        2. Lead block of 2 in. x 4 in. x 8 in.
        3. Aluminum rail for detector and sample holder
        4. Wood
        5. Concrete block of 4 in. x 8 in. x 16 in.
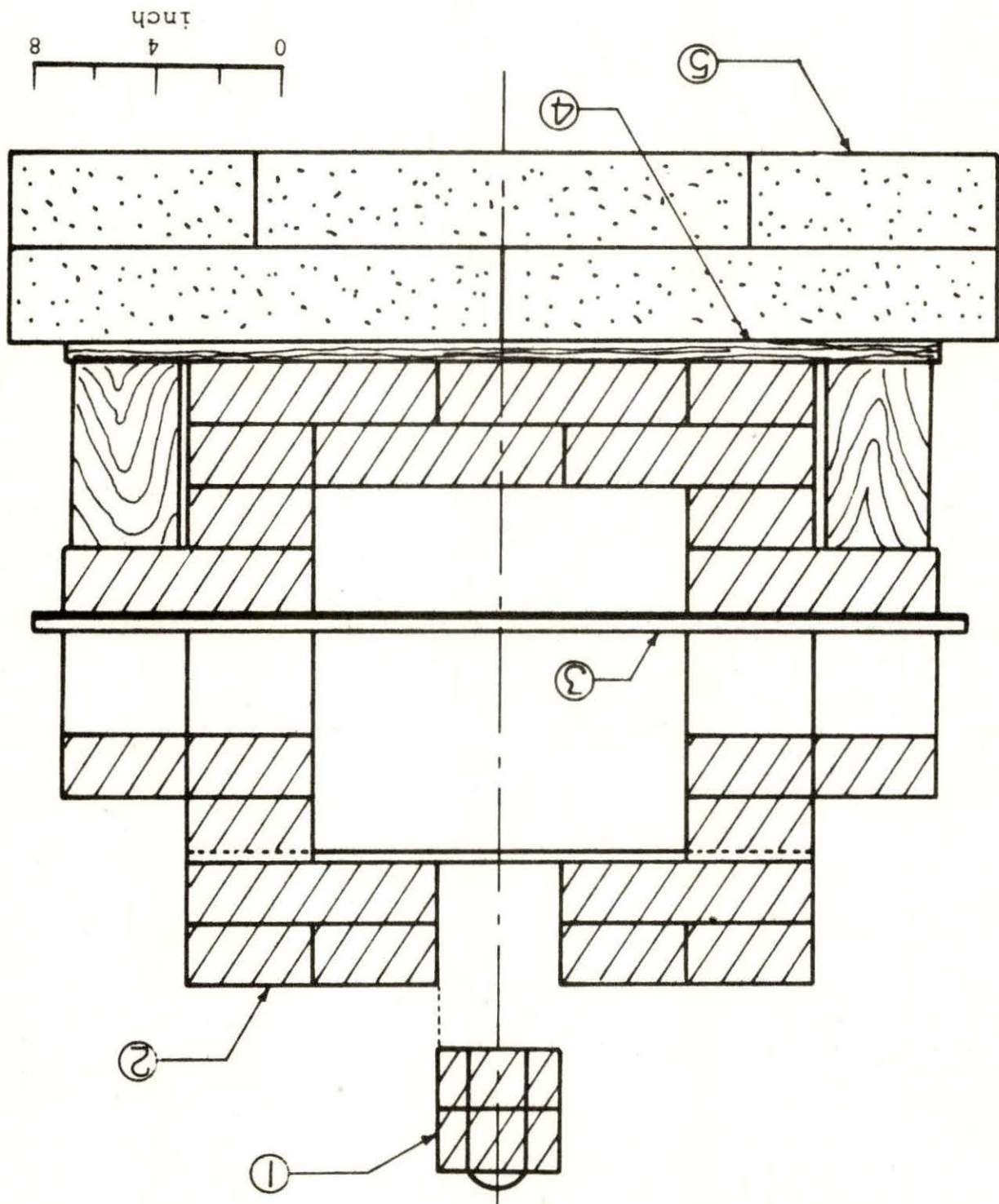
inch

8 4 0

Figure 7. Sample holder for counting

        1. position of disk-shaped sample foil
        2. movable part
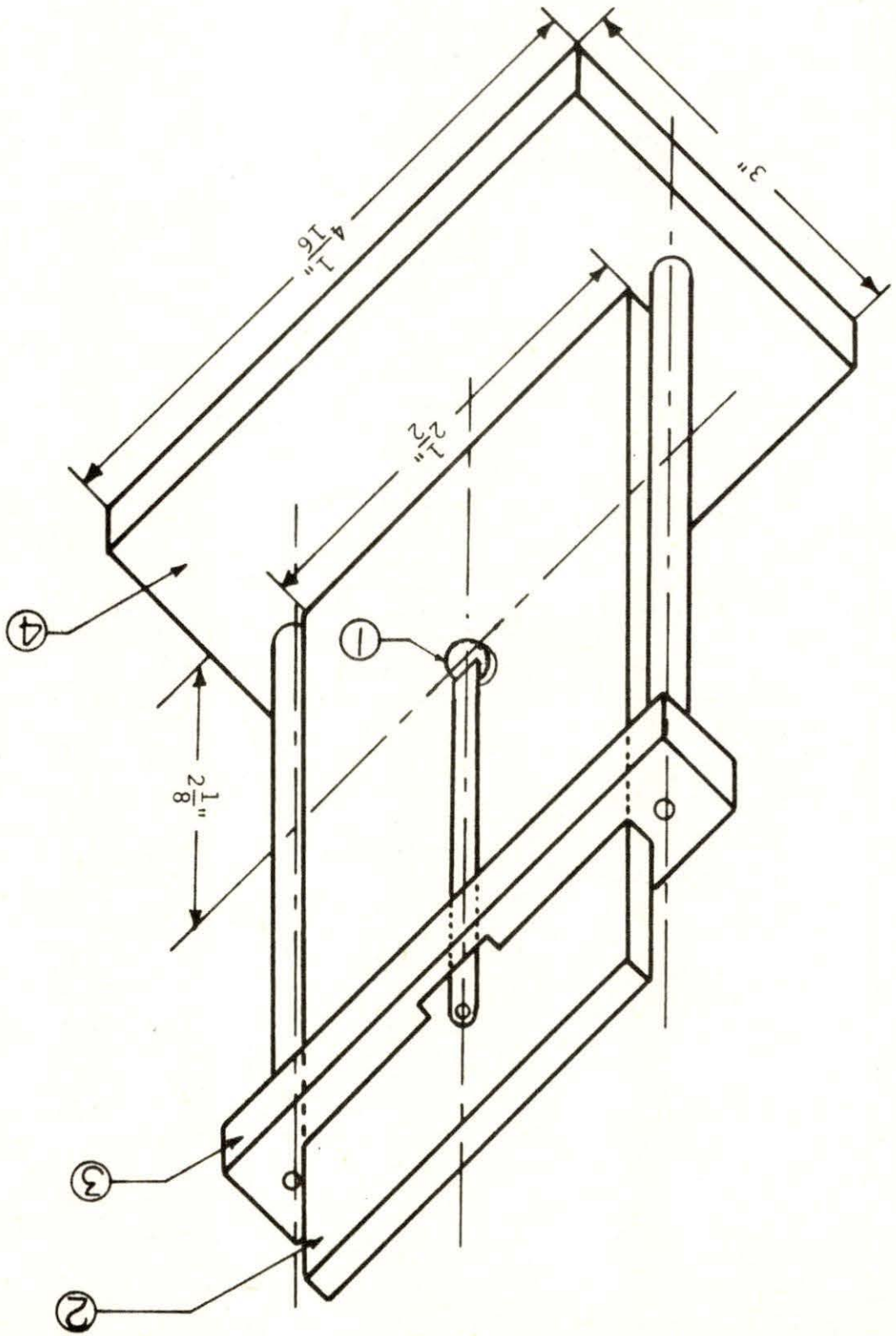   3. fixed frame
        4. base

38

Figure 8. Block diagram of radiation measurement system
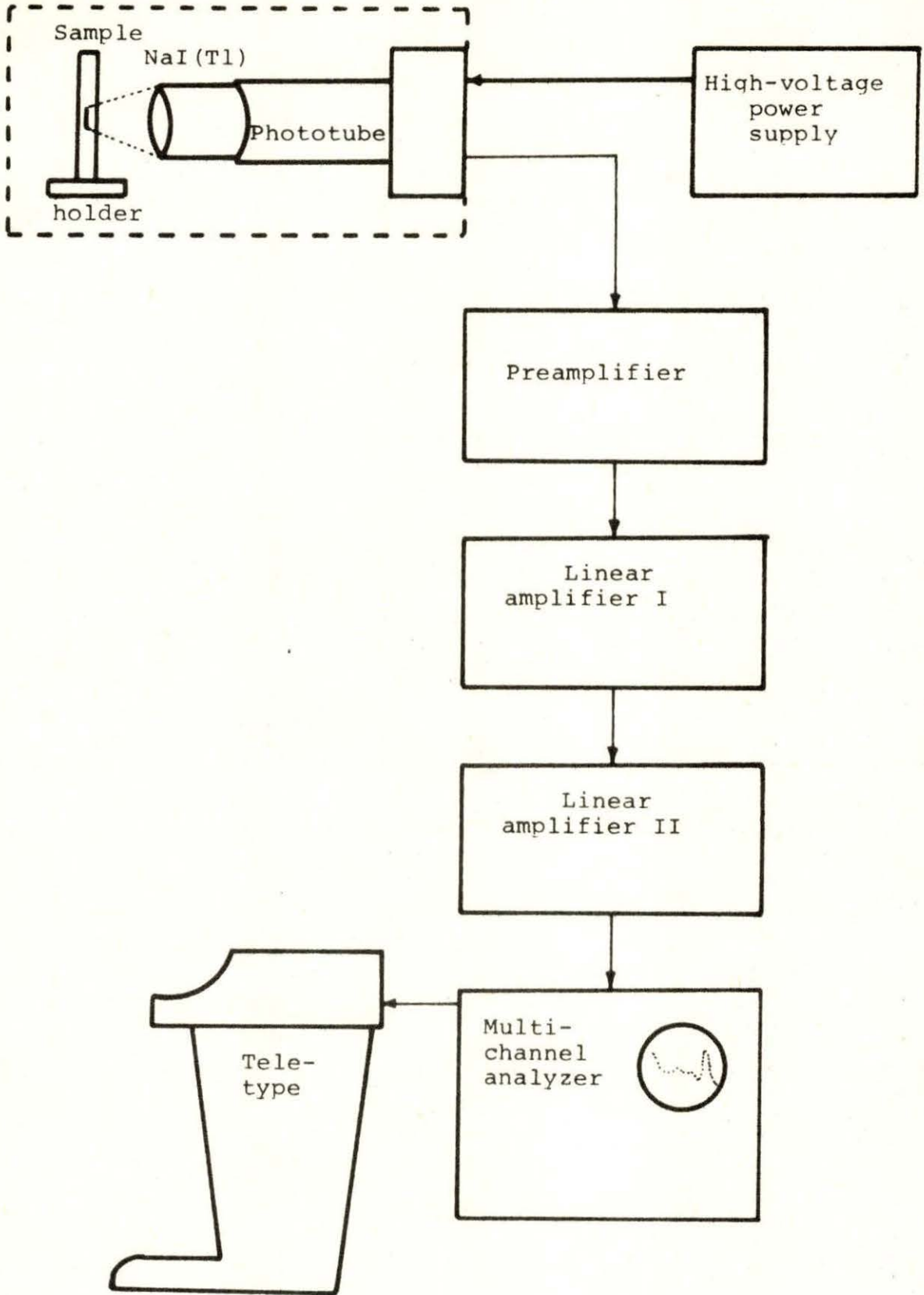(c.f., Table 4)

Table 4. List of equipment for radiation measurements

Name of Instrument	Made by	Model #
1. Multi-channel analyzer	Radiation Instrument Development Lab.	34-12B
2. Timer system	Radiation Instrument Development Lab.	88-901
3. Pulse height analyzer	The Victoreen Instrument Company	PIP-400
4. Teletype printer with punch and reader	The Victoreen Instrument Company	TT-33TC
5. High voltage DC power supply (2)	John Fluke Mfg. Co., Inc.	405B 412B
6. Spectroscopy amplifier (2)	Canberra Industries	816
7. Scintillation preamplifier (2)	Canberra Industries	805
8. Single channel analyzer	Canberra Industries	830
9. Voltage divider (2)	Locally made	
10. NaI(Tl) scintillation crystal with photo-multiplier, "Integral Line", (2)	The Harshaw Chemical Co.	Type-12SS12/E

to increase the counting rate, but the resolution of the photopeak was unacceptably poor. The basic system used was considered to be available in any laboratory engaged in gamma spectra measurements.

Data obtained from the RIDL multichannel analyzer (MCA) and timer system were used to plot the decay curve of In-115m. Two detectors were used in this case since the photopeak width was not an important factor in measuring the decay of the isotope. Whenever energy measurements were performed, the PIP-400 MCA was used. This analyzer was coupled to a teletype console equipped with a paper tape output.

V. EXPERIMENT AND RESULTS

When a sample is irradiated in a gamma field, the flux
distribution throughout the medium of the sample should be
considered. The concept of flux depression factor is help-
ful to do this, and Meghreblian and Holmes (38, pp. 244-
260) discussed flux distribution in foils for the case of
neutrons. Some parts of this theory can be applied to the
case of gamma-rays. For example, by taking their Equation
5.311,

$$\phi(x) = \frac{1}{2} \phi_0 \{E_2(\Sigma_a x) + E_2[\Sigma_a(2a-x)]\}, \quad x \geq 0, \tag{26}$$

where E_2 is the second order exponential integral function,
a is the half-width of a slab with a maximum cross section
Σ_a, and ϕ_0 is the unperturbed flux in the surrounding medium.
By use of this equation, the ratio of the flux at the center
to that at the surface can be approximated by,

$$\frac{\phi(a)}{\phi_0} = E_2(\Sigma_a a) . \tag{27}$$

To depress the flux more than 1% (i.e., $\phi(a)/\phi_0 = 0.99$), the
minimum value of $\Sigma_a a$ should be 0.001. In the case of
In-115(γ,γ')In-115m reaction, the activation cross section
of this reaction is of the order of $10^{-32} cm^2$ (15, 18, 21),
and the atom density of In-115 is approximately 10^{22}

atoms/cm^3. The minimum thickness of indium foil required to depress the gamma flux more than 1% is of the order of 10^{6}cm. Therefore, the effect of flux depression for gamma irradiation is negligible.

Before pulse height spectra measurements were started, the multichannel analyzer was calibrated at 2 keV/channel by using Cs-137 as an energy standard. The system was adjusted so that the 662 keV gamma photopeak was located in channel number 311. It has been observed that calibration procedures should be applied before each experimental run and that the room temperature should be maintained within a 2-3 degree Centigrade range.

The experimental data were originally obtained from a teletype paper tape printout from the 400-channel memory in the multichannel analyzer. The data on paper tape were then transferred to computer cards through a remote terminal for later analysis with a digital computer.

Computer programs are widely used for the analysis of pulse-height spectra (39-42). In general, these examples should not be applied directly to gamma activation analysis, because they were originally prepared for neutron activation data and usually attempt to unfold complex spectra, thereby using large amounts of computation time. Adapting some techniques from these examples, a computer program, DIRFIT, which will be discussed in Appendix C, was written for

fitting the Gaussian function to photopeak data by the least squares method. This computer program includes subtraction of background, calculation of the total area under the photopeak, time corrections, calculation of the specific count rate, and statistical calculations.

A. Analysis of Indium

Indium contains two isotopes which have metastable states in nature, In-113 and In-115, with abundances of 4.3% and 95.7% respectively (22). Table 1 is a list of these data in detail. Thus, two photopeaks can be seen in the pulse-height spectrum of the indium gammas after sufficiently long irradiation. The energies of gamma rays are 393 keV and 355 keV from In-113m and In-115m respectively, so their photopeaks are located close to each other in the pulse-height spectrum. The activity of the 395 keV component is approximately 6% of that of the 355 keV component at the saturation activity based on the assumption that both activation cross sections are the same. Their half lives are 100 min. and 4.5 hr. for In-113m and In-115m, respectively. Therefore, the photopeak of In-115m includes very little activity of In-113m except around the higher energy foot of the peak (c.f., Figure 9).

The decay scheme of In-115 is shown in Figure 10. The nucleus of In-115 decays to its ground state by gamma

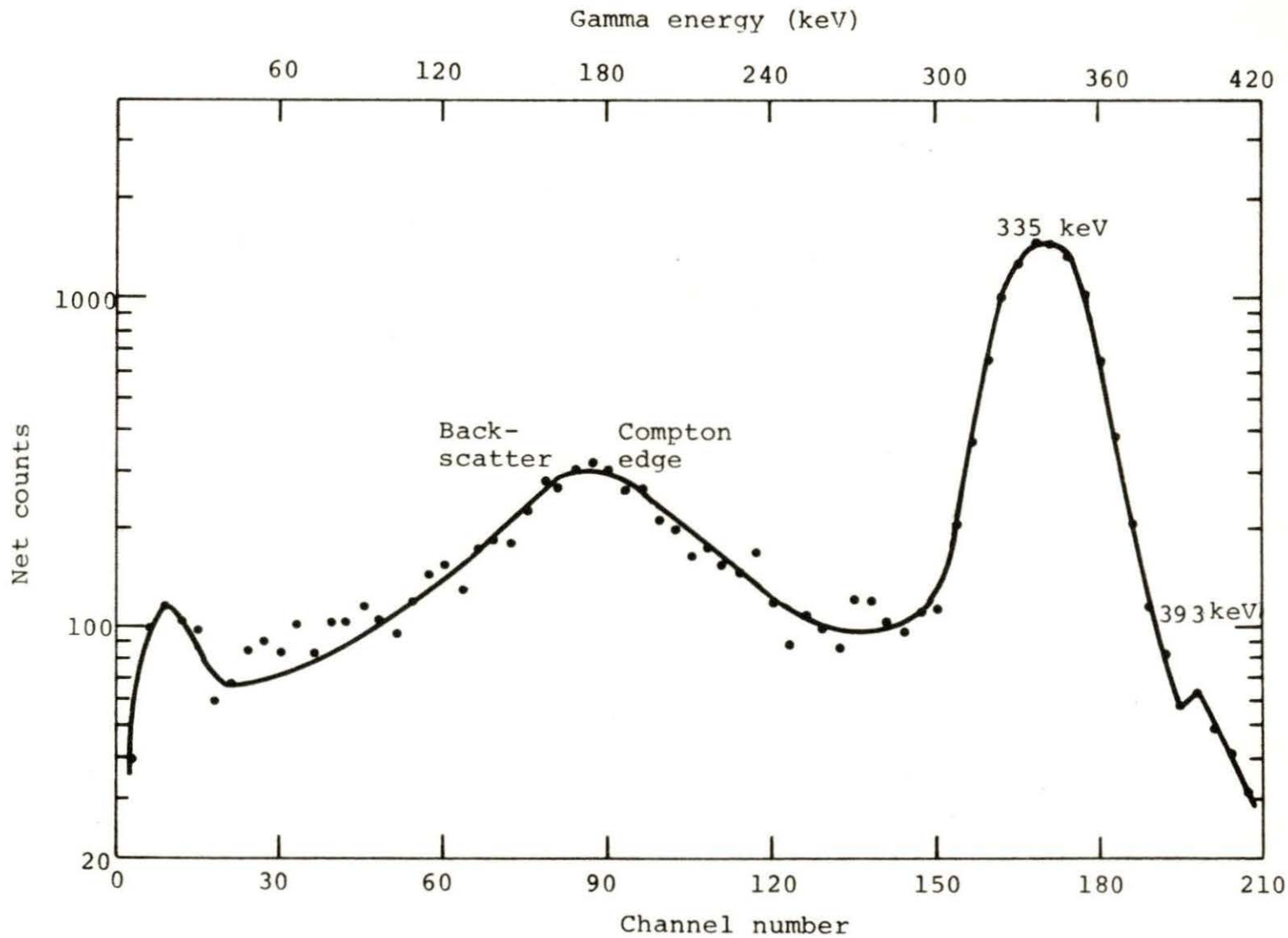Figure 9. Pulse-height spectrum of indium (The original data were modified
by a three-point arithmetic-mean smoothing program)

$t_i \simeq 50$ hours

$t_w = 5$ mins.

$t_c = 80$ mins.
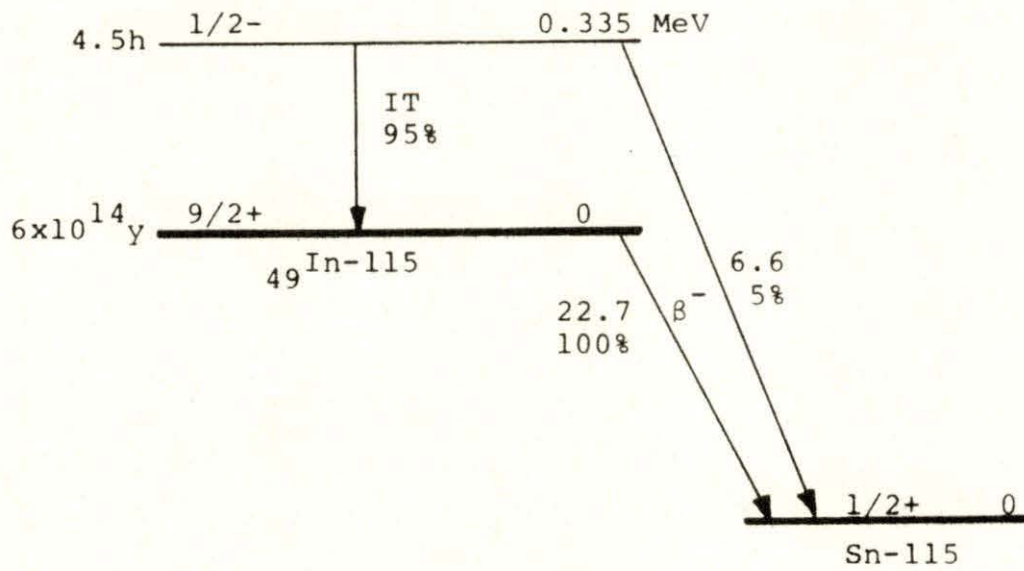
Sample mass = 2379.8 mg.
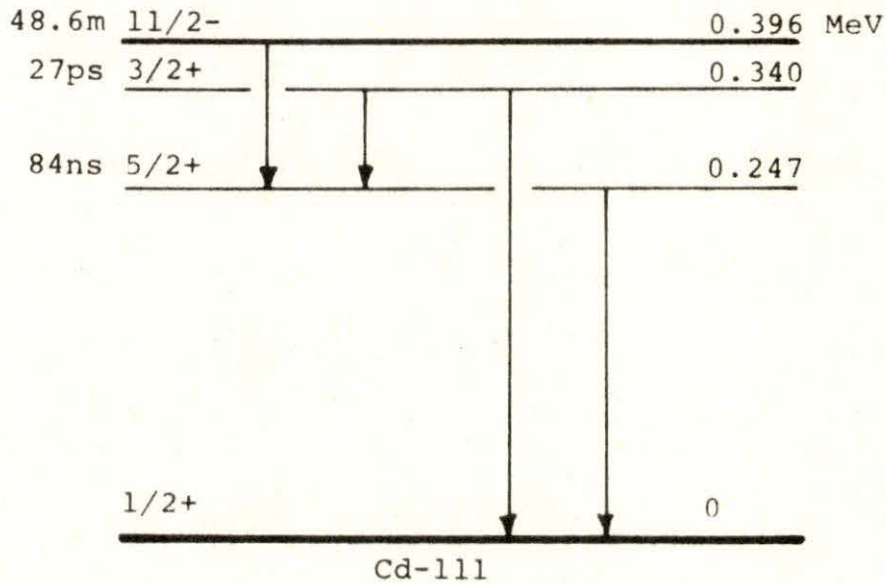
47

48

Figure 10. Decay scheme of In-115m (22)

Figure 11. Decay scheme of Cd-111m (22)

transition with 95% probability and to the ground state of Sn-115 by beta emission with 5%. The former decay procedure is called isomeric transition (IT), and the latter is beta-decay (β^-). Data of probability P_γ of gamma-ray emission, internal conversion coefficient and calculated Compton edge and backscattered-gamma energies for In-115m and Cd-111m are listed in Table 5.

Samples of indium were disk shaped with half-inch diameter. The mass of one foil was approximately 100 mg. About 20 foils were irradiated in the Co-60 gamma irradiation facility at the same time. The case of irradiation of very thick samples was considered and uniform activation throughout was expected.

Sample foils were held in a brass tube (5/8 inch diameter) in the irradiation facility. Its location was shown in Figure 5. The irradiation time of indium was about two days; this time was approximately equal to 10 times the half-life of 4.5 hours of In-115m. This time of irradiation can be expected for In-115 to produce saturation activity.

The half-life of In-115m is given as 4.48 - 4.53 hours (22), but these values are not precise enough to use for time correction in the order of one minute. Therefore, the half-life of In-115m was measured very carefully as one of the parts of this investigation.

A two-gram sample of indium was irradiated for two days

Table 5. Data with respect to gamma energy emitted from In-115m and Cd-111m

Isomer	E_γ (keV)	P_γ	α	e_k/γ	$e_k/(e_T-e_k)$	E_B (keV)	E_C (keV)
I-115m	335	50%	1.005	0.8	3.8	145	188
Cd 111m	149.6	30%	2.25	1.5	2.0	94.3	55.3
	246	94%	0.055	0.054	5.1	125	121

E_γ = energy of photon (22)

P_γ = probability of photon production (22) and calculated with
P_γ = P(IT)/(1+α)

α = internal conversion coefficient and defined as $\alpha = e_T/\gamma$

e_T = the number of total internal conversion electrons

γ = the number of gamma quanta emitted

e_k = the number of internal conversion electrons in the k shell

E_B = energy of back scattered photon, and calculated with
$E_B = E_\gamma/(1+2E_\gamma/E_e)$, where E_e = 510 keV

E_C = energy of Compton edge, and calculated with $E_C = E_\gamma - E_B$

and then placed between two 3- by 3- inch NaI detectors. Amplified pulse-height signals passed through a single-channel analyzer before being stored in a pulse height analyzer operating as a multiscaler with 100-second counting time in each of 400 channels.

The indium decay data are plotted in Figure 12. All of the data could not be used to fit a linear curve on a semi-log graph, because the activity near the time origin included contributions from In-113m. However, data obtained 4 hours after the end of the irradiation could be used. At that time, the component of the observed activity originating from the decay of In-113m was less than 2% of the total activity, so the counts after that time corresponded to the decay of In-115m.

To fit a linear function to the natural logarithm of the data, the OMNITAB (43) computer program was used. OMNITAB fits the data based on the least squares method and gives values of the constants, a and b, with their standard deviations, of an equation of the form,
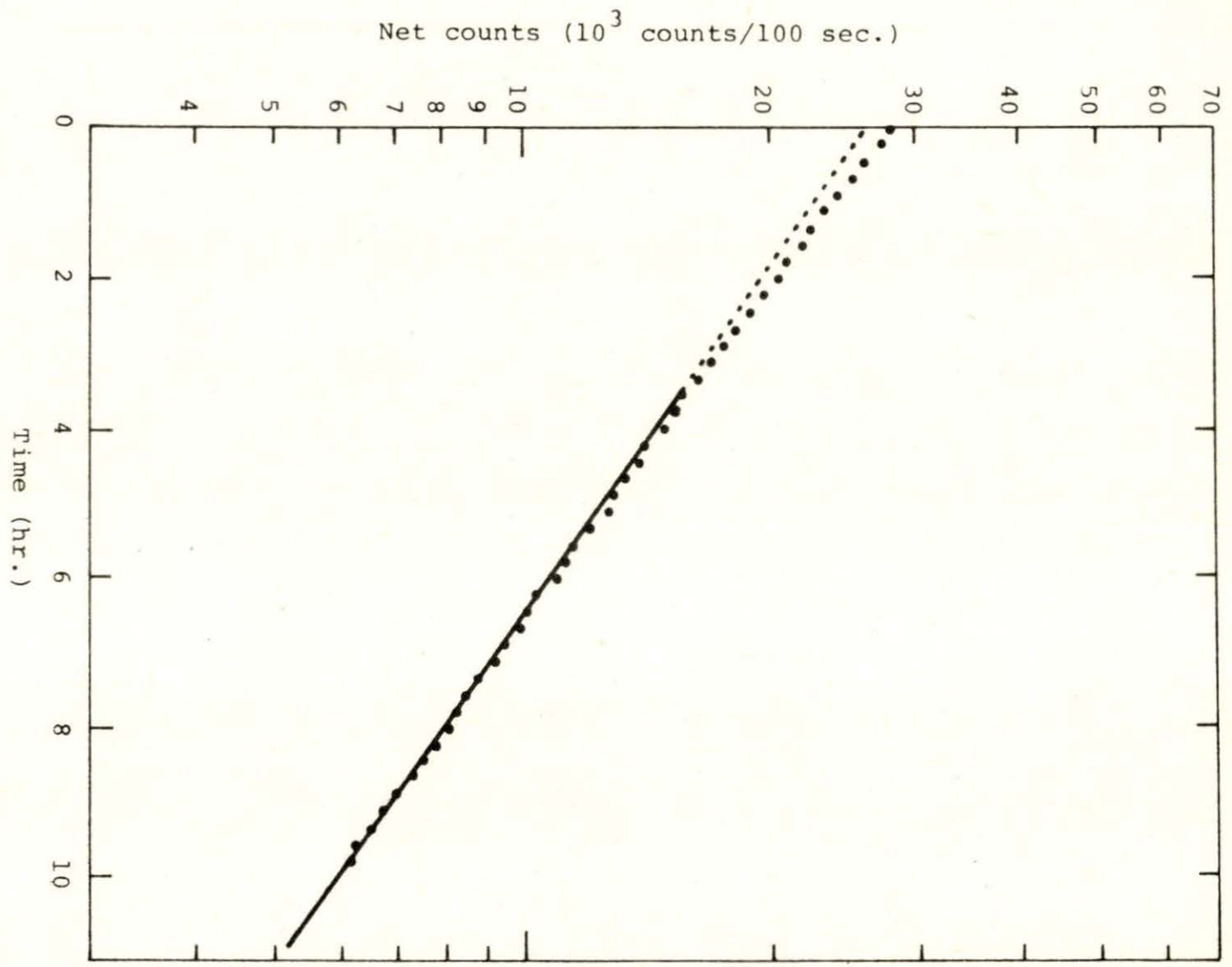
$$y = at + b, \tag{28}$$

where y is $\ln A(t)$, b is $\ln A_s$, a is $-\lambda$, and t is the time.

The measured half-life on In-115m was calculated with the aid of OMNITAB to be

Figure 12.   Decay curve of In-115m

Two 3- by 3-inch NaI detectors,

$t_i \simeq 30$ hours,

$t_w = 10$ mins.,

Sample mass = 2,379.6 mg.

53

$$T_{1/2} = 274.68 \pm 0.67 \text{ mins.}$$

$$= 4.578 \pm 0.012 \text{ hrs.}$$

(29)

The error values are expressed as

$$\Delta T_{1/2} = \sigma t_{0.99} ,$$

(30)

where σ is the standard deviation of $T_{1/2}$, and $t_{0.99}$ is the "student-t" value for the 99% confidence interval. For this case, $t_{0.99} = 2.576$ (31).

The half-life values reported by other investigators are briefly reviewed in the interest of providing a basis for comparison. Salisbury and Chalmers (44) used the In-115(n,n')In-115m reaction to obtain a value of $T_{1/2} = 4.48$ hours. A value of 4.50 hours was obtained by Lawson and Cork (45). Very little information concerning the details of the measurements was available.

A counting program was designed to fulfill the objectives that the least statistical error would be encountered in a reasonable counting period for five samples. Since background fluctuation is a nontrivial factor in low activity measurements, the background activity was measured before the first sample, between each of the five samples, and at the conclusion of the counting period. A balance between reasonable statistical precision gained through large population sampling and the need to finish the measurements before

the fifth sample activity was too low, led to the adoption
of the following program for indium; background count - 10
minutes, sample count - 20 minutes, background count - 10
minutes, etc.

All data are listed in Tables E-1 and E-2 in Appendix E,
and the data of count rate for various masses of indium are
plotted in Figure 13. A mean value of the specific count
rate (i.e., the slope of the straight line in Figure 13)
was calculated in Appendix A by taking 12 values of indium
data, and the result is

Specific count rate of In = 2.395 $\pm$ 0.019 cpm/mg. (31)

It must be emphasized that this specific count rate is based
upon the area of a Gaussian function fitted to the photo-
peak and not the total activity.

B. Analysis of Cadmium

The cadmium isotope of interest was Cd-111m, which decays
with a half-life of 48.6 minutes (22). Since the Cd-111m
half-life is considerably shorter than that of In-115m, the
experimental measurement techniques were adjusted accordingly.
The irradiation time was decreased to 8 hours for cadmium
and only one foil sample was removed from the irradiator for
activity measurement. Waiting time was decreased to a
practical minimum value of two minutes, which was the time

Figure 13.   Count rate vs. mass of In-foil   (The numbers
             in the graph are the datum numbers found in
             Table E-3.   The slope of the line was calculated
             in Appendix A with 11 data points)
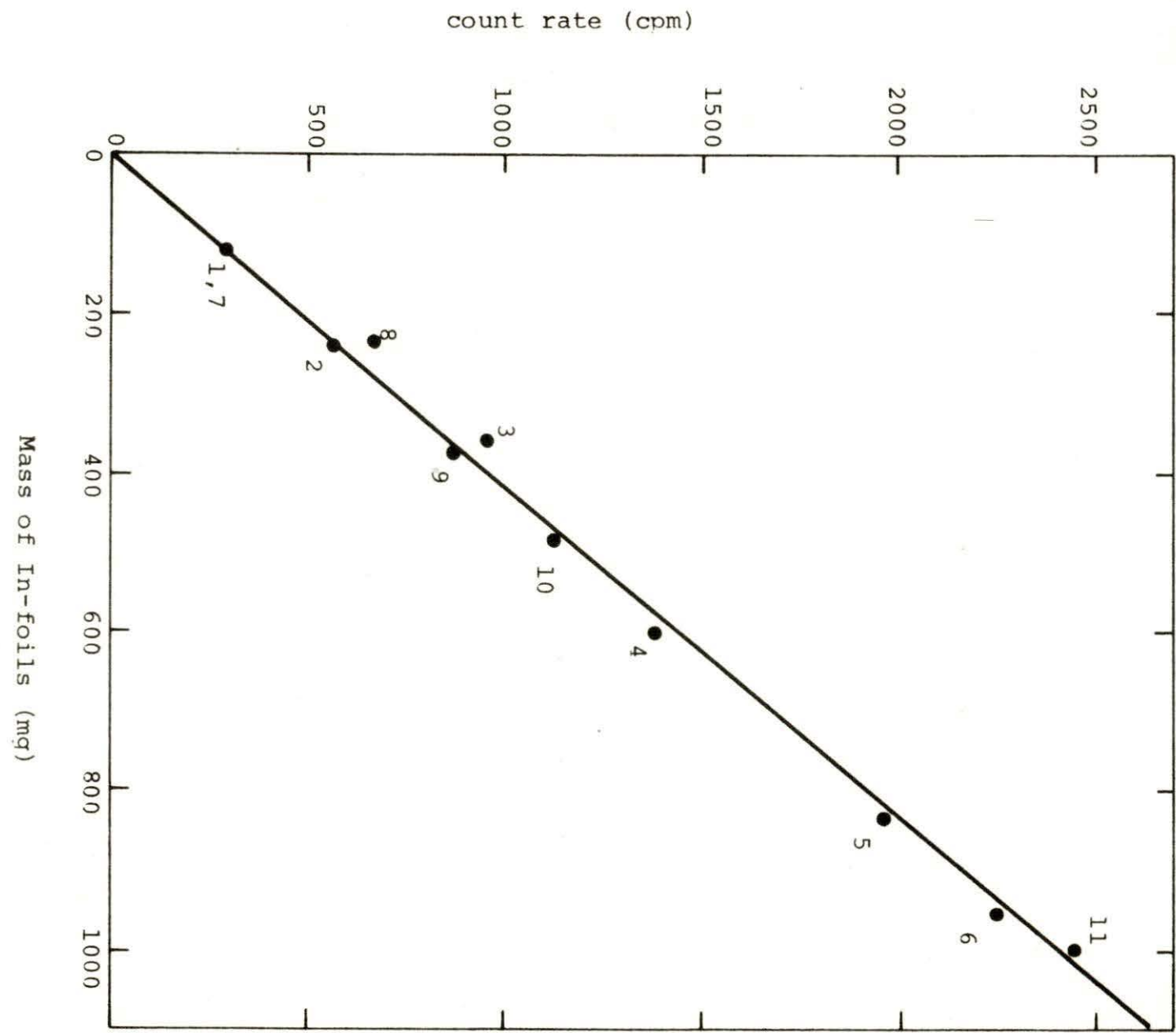
necessary for transport from irradiator to counter.

The decay scheme of cadmium-111m, illustrated in Figure 11, shows a 149 keV transition from the isomeric state to the 247 keV level followed by an "immediate" decay to the ground state, and that the decay proceeds by isomeric transition, only. These two gammas are detected (c.f., Figure 14 and Table 5) with higher efficiency in NaI than the higher energy indium gammas, however, the difference is not of practical consequence in this case.

The anticipated low activity levels of cadmium caused a revision in the counting program so that counts were accumulated until the sample activity decreased to background level. Twenty- and forty-minute counting intervals were tried, with the forty-minute period preferred. Ten-minute background counts before and after the sample measurement were used as before.

All data are listed in Tables E-3 and E-4 in Appendix E, and the count rates for various masses of cadmium are plotted in Figure 15. A mean value of the specific count rate (i.e., a slope of the straight line in Figure 15) is calculated in Appendix A by taking 7 values of cadmium data, and the result is

Specific count rate of Cd = 0.2307 $\pm$ 0.0008 cpm/mg.   (32)

Figure 14.   Pulse-height spectrum of cadmium (The data
              corresponds to No. 7 of cadmium, (c.f., Table
              E-3). The original data were modified by a
              three-point arithmetic-smoothing program)

              t_i ≃ 20 hours,

              t_w = 4 mins.,

              t_c = 40 mins.,

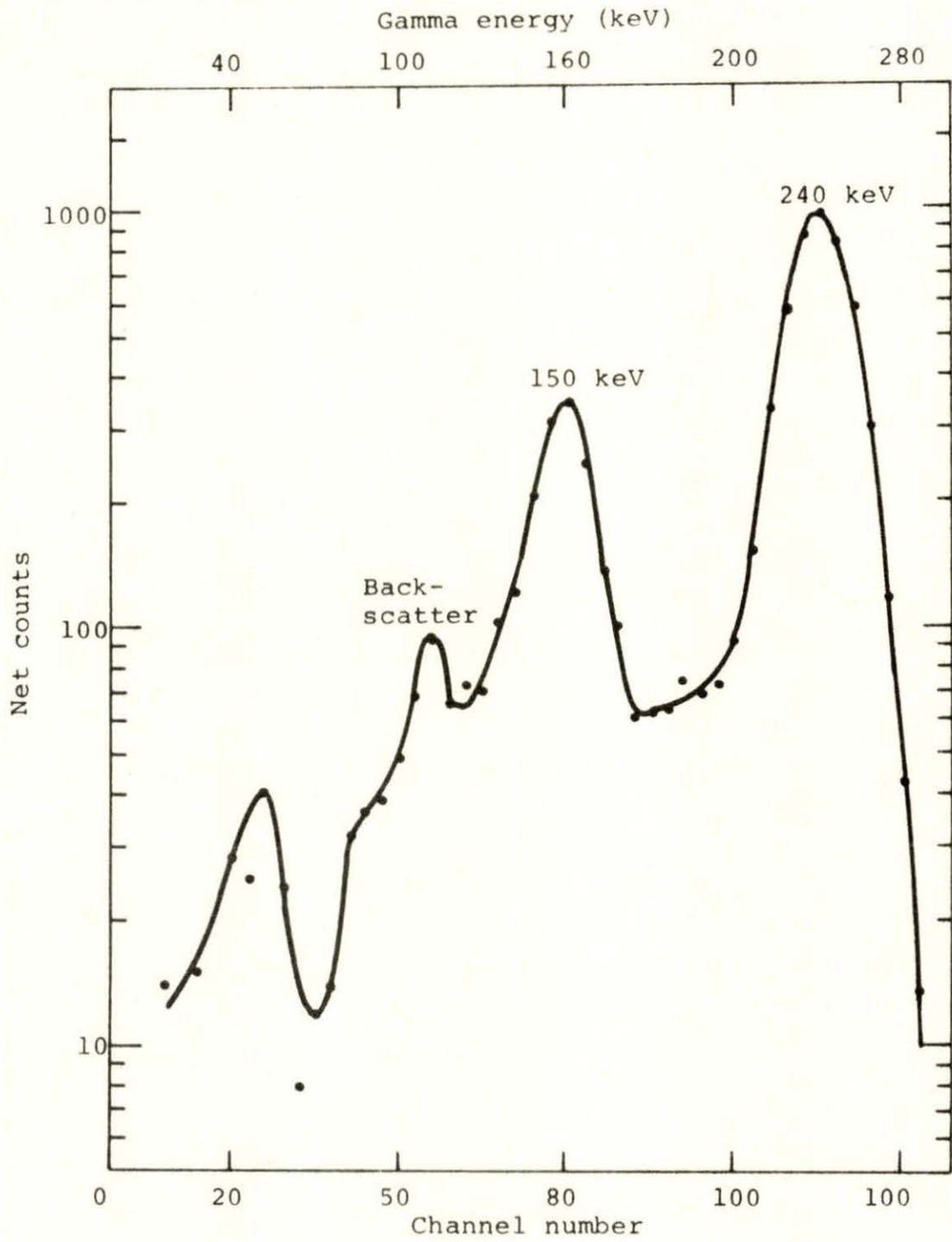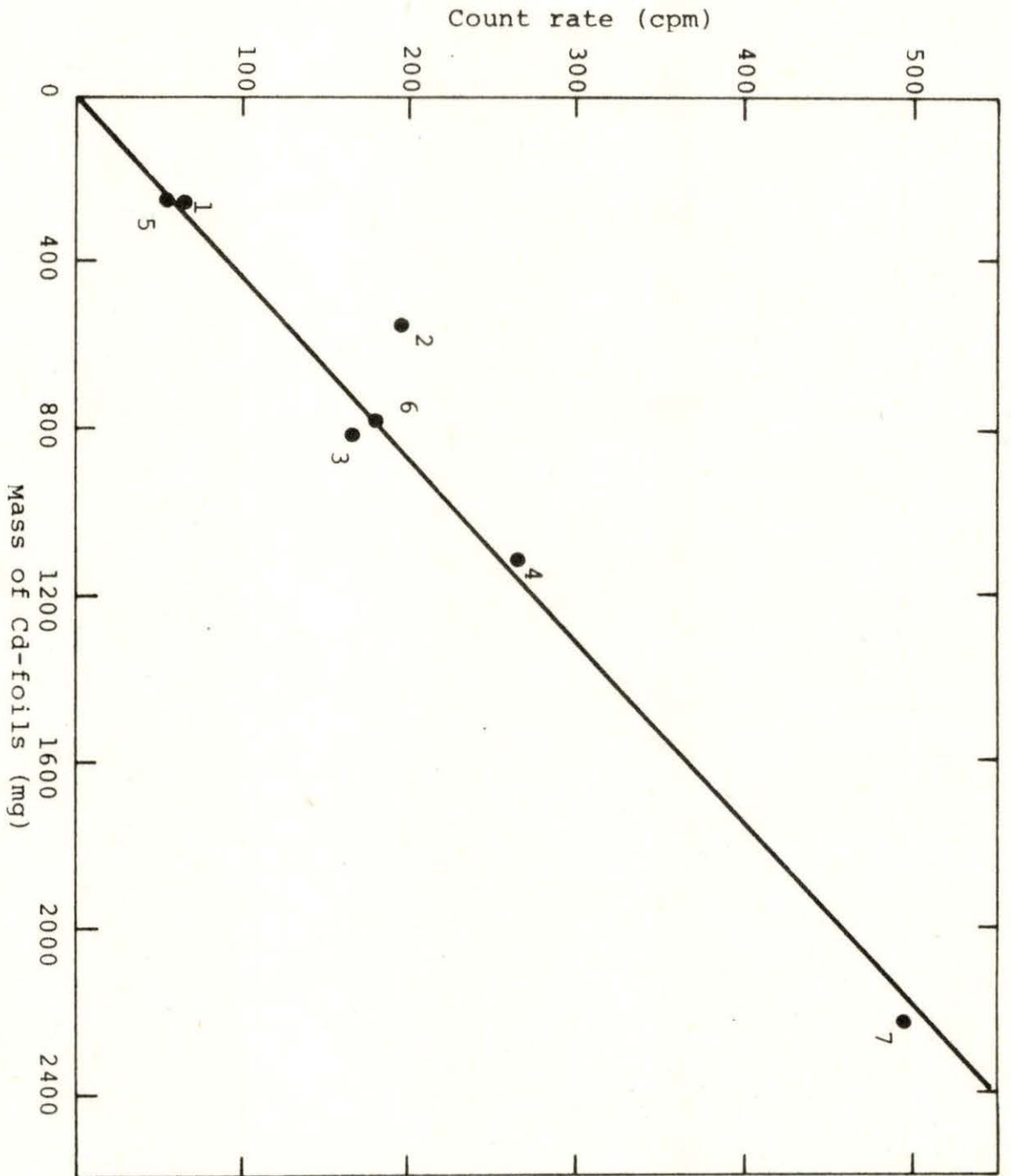   Sample mass = 2234.0 mg.

Figure 15. Count rate vs. mass of Cd-foil (The numbers in the graph are the
            datum numbers found in Table E-3. The slope of the line was
            calculated in Appendix A)

As before, this rate is based on the photopeak fitted Gaussian area.

With the activation cross section of the Cd-111(γ,γ') Cd-111m reaction approximately 1.2×10^{-32} cm^2, the natural abundance of the isotope at 12.7%, and $P_\gamma = 0.94$ for the 246 keV-gamma (c.f., Table 5), the expected specific counting rate of cadmium would be about seven times lower than the indium rate under equivalent experimental conditions. This compares favorably with the experimental observations of 2.395 cpm/mg and 0.2307 cpm/mg for indium and cadmium, respectively.

The minimum detectable amount of indium or cadmium activated by Co-60 gamma-rays depends on many factors; some of the factors are:

(1)   intensity of Co-60 source,

(2)   magnitude of the background,

(3)   detection efficiency of the measurement system,

(4)   time table of the measurements, such as counting time for source counts and background, and waiting time,

(5)   natural abundance of the nuclear isomer,

(6)   half-life of the isomeric state,

(7)   activation cross-section,

(8)   gamma emission probability,

(9)   complexity of the decay scheme of the nuclear
      isomer,

(10) maximum allowable value of the estimated standard
      error.

By inclusion of all these factors, the absolute values of
the minimum detectable amount could be evaluated, but in
practice, it would be very difficult. Therefore, to calcu-
late a reasonable value of the minimum detectable amount,
some specific conditions should be stated; furthermore, it
does not follow that any of the conditions are absolute
standards, but they can be chosen with the aid of experience.
The following three conditions were employed:

(1)   The counting time for background is one-half
      of that for the source count.

(2)   The maximum standard error of the total count is 5%.

(3)   a.   For the analysis of indium, the most reasonable
           waiting and counting times are 5 min. and 20
           min., respectively.

      b.   For the analysis of cadmium, the most reason-
           able waiting and counting times are 2 min.
           and 40 min., respectively.

In addition to the three previous conditions, the specific
count rates were determined under the following experimental
and analytical conditions:

(1) The dose rate of the Co-60 source was approximately 10^4 rad/min.

(2) The distance between the one-half inch diameter sample foil and the surface of the 3 in. x 3 in. NaI crystal was 1.1 cm.

(3) The specific count rate and its uncertainty were determined from a Gaussian function fitted to photopeak data. Measured foil masses were assumed to have negligible error.

The minimum detectable amounts (or sensitivities) and the precision of the gamma activation analysis of indium and cadmium with Co-60 gamma-rays are:

Indium: 18.3 ± 2.4 mg.

Cadmium: 117.0 ± 15.2 mg.

The uncertainties are calculated at the 99% confidence level based only on the random character of the radioactivity measurements.

VI. CONCLUSIONS

The feasibility of measuring tens-of-milligrams amounts of indium and cadmium by gamma activation analysis using a Co-60 irradiator has been demonstrated. This method of analysis may not replace other methods, but it should be considered as an alternative if the particular experimental conditions are favorable. Some of the advantages of this method are:

1. Samples can be analyzed non-destructively.

2. Expensive irradiation facilities, e.g., nuclear reactors are not required.

3. Intensive personnel monitoring of the irradiator is not necessary during activation.

4. Commonly available pulse-height analysis systems are sufficient for radiation measurement.

The sensitivity of gamma activation analysis was investigated in terms of the minimum detectable mass. Sensitivity calculations must be based on clearly stated conditions describing the minimum acceptable precision and counting period routines. In addition, the specific count rate (e.g., cpm/mg.), which implicitly contains information about the detection efficiency and the production and loss rates of radioisotope, or its equivalent, must be specified.

Under the conditions of this investigation, indium

and cadmium were detectable at minimum masses of 18.3 $\pm$ 2.4 mg. and 117.0 $\pm$ 15.2 mg., respectively (c.f. Appendix B). These values are smaller than those reported by previous investigators (c.f. Table 2).

The photopeak fitting method was shown to be a valid technique through experimental verification of the linear relationship between measured activity and the sample mass.

Several elements, which are listed in Table 1, are detectable through gamma activation analysis, however, their sensitivities may be higher than those of indium and cadmium. Investigation of mercury and rhodium, for example, should be attempted to determine their sensitivity to gamma activation analysis.

VII. BIBLIOGRAPHY

1. Desoete, D., Gijbels, R. and Hoste, J. Neutron, photon and charged particle reactions for activation analysis. Modern trends in activation analysis II: 699-750. Devoe, James R. ed. Washington, D.C., National Bureau of Standards. 1969.

2. Lukens, H. R., Jr., Otvos, J. W. and Wagner, C. D. Formation of metastable isomers by photoactivation with the Van de Graaff accelerator. International Journal of Applied Radiation and Isotopes 11: 30-37. 1961.

3. Harbottle, Garman. Activation of nuclear isomers by gamma rays. Nucleonics 12, No. 4: 64-67. 1954.

4. Ikeda, Nagao and Yoshihara, Kenji. Radioactivation by the (γ,γ)-reaction I; Activation of rhodium and indium by the use of the cobalt-60 γ-ray source. Radio-isotope 5, No. 1: 11-14. 1957.

5. Ikeda, Nagao and Yoshihara, Kenji. Radioactivation by the (γ,γ)-reaction II: Radioactivation of indium by the use of the 2000 curies cobalt-60 γ-ray source. Radioisotopes 5, No. 2: 11-15. 1957.

6. Ikeda, Nagao and Yoshihara, Kenji. Radioactivation by the (γ,γ)-reaction III: Activation cross-section of $^{115}In(\gamma,\gamma)^{115m}In$ reaction. Radioisotopes 7, No. 1: 11-16. 1959.

7. Ikeda, Nagao and Yoshihara, Kenji. Radioactivation by the (γ,γ)-reaction IV: Theoretical considerations on the activation cross-section of $^{115}In(\gamma,\gamma)^{115m}In$ reaction. Radioisotopes 7, No. 1: 17-22. 1959.

8. Ikeda, Nagao, Yoshihara, Kenji and Mishio, Nariyuki. Radioactivation by the (γ,γ)-reaction V: Radioactivation of silver by the cobalt-60 γ-ray irradiation. Radio-isotopes 7, No. 2: 92-96. 1959.

9. Ikeda, Nagao and Yoshihara, Kenji. Radioactivation by the (γ,γ)-reaction VI: Activation cross-section of ^{111}Cd for $^{111}Cd(\gamma,\gamma)^{111m}Cd$ reaction. Radioisotopes 7, No. 3: 195-199. 1959.

69

10. Ikeda, Nagao, Yoshihara, Kenji and Shimada, Kazuo. Radioactivation by the (γ,γ)-reaction VII: Application of the (γ,γ)-reaction to the γ-ray dosimetry; studies on the relative method by the use of 10 kc cobalt-60 γ-ray source. Radioisotopes 8, No. 1: 17-23. 1960.

11. Ikeda, Nagao and Yoshihara, Kenji. Radioactivation by the (γ,γ)-reaction VII: Activation cross-section of $^{103}Rh(\gamma,\gamma)^{113m}Rh$ reaction. Radioisotopes 8, No. 1: 24-27. 1960.

12. Ikeda, Nagao and Yoshihara, Kenji. Radioactivation by the (γ,γ)-reaction IX: Activation cross-section of ^{87}Sr for $^{87}Sr(\gamma,\gamma)^{87m}Sr$ reaction. Radioisotopes 8, No. 3: 238-241. 1960.

13. Yoshihara, Kenji. Studies on the radioactivation by the cobalt-60 γ-ray source I: General considerations on the radioactivation by the use of a γ-ray source of radioisotope. Isotopes and Radiation 3, No. 4: 276-285. 1960.

14. Yoshihara, Kenji. Studies on the radioactivation by the cobalt-60 γ-ray source II; Consideration on the (γ,γ)-reaction by the use of a non-spherical γ-ray source. Isotopes and Radiation 3, No. 6: 464-471. 1960.

15. Yoshihara, Kenji. Studies on the radioactivation by the cobalt-60 γ-ray source III: Cross-sections of various nuclides for the (γ,γ)-reaction. Isotopes and Radiation 3, No. 6: 472-482. 1960.

16. Yoshihara, Kenji. Studies on the radioactivation by the cobalt-60 γ-ray source IV: Studies on the indium dosimetry. Isotopes and Radiation 4, No. 2: 93-101. 1961.

17. Yoshihara, Kenji. Studies on the radioactivation by the cobalt-60 γ-ray source V: Non-destructive analysis by the (γ,γ)-reaction. Isotope and Radiation 4, No. 2: 102-104. 1961.

18. Veres, A. Photo-activation of cadmium-111m and indium-115m by cobalt-60 irradiation. International Journal of Applied Radiation and Isotopes 14: 123-128. 1963.

19. Veres, A. and Pavlicsek, I. Activation of the nuclear isomer indium-113m by gamma rays of cobalt-60. International Journal of Applied Radiation and Isotopes 17: 69-73. 1966.

20. Veres, A. and Pavlicsek, I. Nuclear photoactivation analysis by means of an 80-kCi ^{60}Co-radiation source. Journal of Radioanalytical Chemistry 3: 25-28. 1969.

21. Law, J. and Iddings, F. A. A study of photoactivation with a ^{60}Co source. Journal of Radioanalytical Chemistry 3: 53-63. 1969.

22. Lederer, C. M., Hollander, J. M. and Perlman, I. Table of isotopes. 6th ed. New York, John Wiley and Sons, Inc. 1968.

23. Watt, D. E. and Ramsden, D. High sensitivity counting techniques. New York, The Macmillan Company. 1964.

24. Baker, C. A. Gamma activation analysis. Analyst 92. No. 1099: 601-609. 1967.

25. Segre, Emilio. Nuclei and Particles. New York, W. A. Benjamin, Inc. 1965.

26. Engelmann, Charles. Activation analysis using photons (Translated title). Microfilm copy. France, Commissariat l'Energie Atomique, Centre d'Etudes Nucleaires CEA. R. 3307. 1967.

27. Glasstone, Samuel and Sesonske, Alexander. Nuclear reactor engineering. Princeton, New Jersey, D. Van Nostrand Co., Inc. 1967.

28. Etherington, Harold. ed. Nuclear engineering handbook. New York, McGraw-Hill Book Co., Inc. 1958.

29. Overman, Ralph T. and Clark, Harbert M. Radioisotope techniques. New York, McGraw-Hill Book Co., Inc. 1960.

30. Heath, R. L. Scintillation spectrometry. 2d ed. Vol. 1. U.S. Atomic Energy Commission Research and Development Report IDO-16880-1 (Idaho, Idaho Operations Office, Atomic Engineering Division). 1960.

31. Steel, Robert G. D. and Torrie, James H. Principles and procedures of statistics. New York, McGraw-Hill Book Co., Inc. 1960.

32. Bevington, Philip R. Data reduction and error analysis for the physical sciences. New York, McGraw-Hill Book Co., Inc. 1969.

33. Price, William J. Nuclear radiation detection. 2d ed. New York, John Wiley and Sons Inc. 1964.

34. Friedlander, Gerhart, Kennedy, Joseph W. and Miller, Julian Malcolm. Nuclear and radiochemistry. 2d ed. New York, John Wiley and Sons Inc. 1964.

35. Hald, A. Statistical theory with engineering applications. New York, John Wiley and Sons Inc. 1952.

36. Carlson, Michael C. J. The effect of gamma radiation on the conductivity of sodium chloride. Unpublished Ph.D. thesis. Ames, Iowa, Library, Iowa State University of Science and Technology. 1968.

37. Jones, Dean C. Gamma radiation effects on the electrical conductivity of pyrolytic boron nitride. Unpublished M.S. thesis. Ames, Iowa, Library, Iowa State University of Science and Technology. 1969.

38. Meghreblian, Robert V. and Holmes, David K. Reactor analysis. New York, McGraw-Hill Book Co., Inc. 1960.

39. Heath, R. L., Helmer, R. G., Schmittroth, L. A. and Cazier, G. A. The calculation of gamma-ray shapes for sodium iodide scintillation spectrometers. U.S. Atomic Energy Commission Research and Development Report IDO-17017 (Idaho, Idaho Operations Office, Atomic Energy Division). 1965.

40. Korthoven, P. J. M. Resolf, a computer program for the analysis of gamma-ray spectra. U.S. Atomic Energy Commission Research and Development Report IS-1811 (Ames, Iowa, Ames Laboratory, Iowa State University). 1969.

41. Haustein, P. E. Control card and data input format for "ICPEAX-IV" (The improved version of the automatic photopeak detection program). Private paper. Ames, Iowa, Ames Laboratory, Iowa State University. 1969.

42. Putnum, Marie, Helmer, R. G., Heath, R. L. and Gipson, D. H. Non-linear least squares program for the determination of parameters of photopeaks by the use of a modified Gaussian function. U.S. Atomic Energy Commission Research and Development Report IDO-17015 (Idaho, Idaho Operation Office, Atomic Energy Division). 1965.

43. Hilsenrath, J. OMNITAB, a computer program for statistical and numerical analysis. Washington, D.C., National Bureau of Standards Handbook 101. 1966.

44. Salisbury, S. R. and Chalmers, R. A. Fe^{54} (n,p), (n,α), and (n,2n) cross sections. Physical Review 140, No. 2B: B305-B310. 1965.

45. Lawson, J. L. and Cork, J. M. The radioactive isotopes of indium. Physical Review 57, No. 11: 982-994. 1940.

VIII. ACKNOWLEDGMENTS

I would like to thank Dr. Richard A. Hendrickson, my major professor, for his valuable advice throughout this research and for helping me with my language difficulties.

I would also like to thank the other members of my committee, Dr. Glenn Murphy, Dr. Paul W. Barcus, and Dr. Willard L. Talbert, Jr. for their kind encouragement. In particular, I would like to thank Dr. Glenn Murphy, Head of Nuclear Engineering Department, for making financial assistance available and for his frequent and helpful advice concerning all aspects of my graduate program.

Finally, I would like to thank my wife for her help, and our parents for their sending encouraging letters from Japan.

IX. APPENDIX

A. Calculation of Specific Count Rates

It is necessary to calculate a mean value of the specific count rate (i.e., the slope of the lines in Figures 13 and 15) of the experimental data. In this case, the mean value can not be simply calculated by summing of the data and dividing by the number of points, because each has unequal uncertainty. A method of estimation of the mean for the case of unequal uncertainties was given by Bevington (32), and his Equations 5-14 and 5-15 are applied to this calculation.

Let μ and μ_i be defined as the mean value of specific count rate and the individual specific count rate of indicated datum i; the mean μ is given by

$$\mu \simeq \frac{\sum\limits_{i=1}^{n} \mu_i/\sigma_i^2}{1/\sigma_i^2} , \qquad (A-1)$$

where σ_i is the uncertainty of μ_i, and also the uncertainty σ_μ of μ is given by

$$\sigma_\mu^2 \simeq \frac{1}{\sum\limits_{i=1}^{n} 1/\sigma_i^2} . \qquad (A-2)$$

Thus, the results are

In: $\mu \pm \sigma_\mu t_{0.99}$ = 2.395 $\pm$ (0.006)(3.106)

$$= 2.395 \pm 0.019 \text{ cpm/mg}, \qquad \text{(A-3)}$$

Cd: $\mu \pm \sigma_\mu t_{0.99}$ = 0.2307 $\pm$ (0.0002)(3.707)

$$= 0.2307 \pm 0.0008 \text{ cpm/mg}. \qquad \text{(A-4)}$$

The data number 12 of indium was omitted from this mean value calculation. When that datum was included, the mean value was $\mu = 2.295 \pm 0.019$ cpm/mg. Thus 4% difference seems to be caused by μ_{12} being very small when compared with other values (i.e., $\mu_{12} = 2.02$ cpm/mg and arithmetic mean of 11 values is 2.43 cpm/mg; c.f., Table E-1) and the weighting factor of μ_{12} being especially large (i.e., small σ_{12}).

It can be considered that functions of self-absorption in the measurement and scattering in the irradiation are not negligible in a thick medium such as No. 12 indium sample. Because of these reasons, μ_{12} should be omitted from the data which are used for calculation of the mean value of the specific count rate. Further measurements in the neighborhood of 2,000 mg would be necessary to verify these considerations.

B. Calculation of the Minimum Detectable Amount

To simplify the calculations in this section, the following symbols are used:

S = total counts including background for counting

   time, t_s,

B = background counts for counting time, t_b,

N = net counts per time, t_s, and

σ_N = standard deviation of the value of N.

If the background is steady through the measurements, the relationship among the variables, S, B, and N must be

$$N = S - (\frac{t_s}{t_b})\, B. \tag{B-1}$$

The standard deviation, σ_N will be derived by a general method as follows:

$$\sigma_N \simeq t_s \sqrt{\frac{S}{t_s^2} + \frac{B}{t_b^2}}$$

$$= \sqrt{S + (\frac{t_s}{t_b})^2 B}\,. \tag{B-2}$$

For calculation of the standard deviation, it is not necessary to consider time correction, since uncertainty of time is assumed to be negligible. By substituting Equation B-1 for S in Equation B-2, σ_N is also given by

$$\sigma_N \simeq \sqrt{N + (\frac{t_s}{t_b})B + (\frac{t_s}{t_b})^2 B}\,. \tag{B-3}$$

Let δ be the standard error of σ_N for N, and then

$$\delta = \frac{\sigma_N}{N} \ .$$ (B-4)

With Equation B-3, this error is

$$\frac{\sigma_N}{N} \simeq \sqrt{\frac{1}{N}[1 + (\frac{t_s}{t_b})\frac{B}{N} + (\frac{t_s}{t_b})^2 \frac{B}{N}]} \ .$$ (B-5)

The condition for minimum error was discussed by Price (33). Equation 3-30 as used by him can be applied here. With the symbols of this section,

$$\frac{t_b}{t_s} \simeq (\frac{B/t_b}{S/t_s})^{\frac{1}{2}} \ .$$ (B-6)

Rearrangement gives

$$\frac{B}{S} \simeq (\frac{t_b}{t_s})^3 \ .$$ (B-7)

Now, to investigate the minimum detectable amount, some conditions must be stated. Specific examples are cited.

(1) The counting time for background is half that of the source, i.e.,

$$\frac{t_b}{t_s} = \frac{1}{2} \ .$$ (B-8)

(2) The maximum percentage standard error is chosen as 5%, i.e.,

$$\delta_o = \frac{\sigma_{No}}{N_o} = 0.05. \tag{B-9}$$

The values used with the conditions are symbolized with subscript o. With condition 1, Equation B-1 is

$$N_o = S_o - 2B_o, \tag{B-10}$$

and Equation B-6 is

$$\frac{B_o}{S_o} = \frac{1}{8}. \tag{B-11}$$

Therefore, with these values, Equation B-5 is given as

$$\frac{\sigma_{No}}{N_o} = \sqrt{\frac{2}{N_o}}. \tag{B-12}$$

From condition 2, the value of N_o can be calculated as follows:

$$\sqrt{\frac{2}{N_o}} = 0.05,$$

$$N_o = 800 \text{ counts.} \tag{B-13}$$

The value of N corresponds to that of C_T defined in Equation 8, therefore, to calculate the saturated count rate, R, with Equation 9, some more conditions are necessary here. Those are:

(3) a. for indium, the waiting and counting times are

taken as

$$t_w = 5 \text{ mins.},$$

$$t_c = 20 \text{ mins.}, \qquad \text{(B-14)}$$

b. for cadmium,

$$t_w = 2 \text{ mins.},$$

$$t_c = 40 \text{ mins.} \qquad \text{(B-15)}$$

For those counting times, the minimum saturated count rates R_o are

In: $R_o = (800)(0.0521) = 42 \text{ cpm},$ (B-16)

Cd: $R_o = (800)(0.0337) = 27 \text{ cpm},$ (B-17)

where the values of 0.0521 and 0.0337 are time correction factors calculated with Equation 9. These values have 5% standard error because of condition 2, and for these values, the "student-t" value for the 99% confidence interval is $t_{0.99} = 2.576$.

Thus the minimum detectable saturated count rate can be written with values of relative standard error as follows:

In: $R_o = 42 \pm 5.4 \text{ cpm},$ (B-18)

Cd: $R_o = 27 \pm 3.5 \text{ cpm}.$ (B-19)

With values of specific count rate estimated in Appendix A, the minimum detectable amounts are calculated as follows:

In: $\dfrac{42 \pm 5.4 \ (cpm)}{2.295 \pm 0.019 \ (cpm/mg)} = 18.3 \pm 2.4 \ mg,$ (B-20)

Cd: $\dfrac{27 \pm 3.5 \ (cpm)}{0.2307 \pm 0.0008 \ (cpm/mg)} = 117.0 \pm 15.2 \ mg.$ (B-21)

C. Computer Program
DIRFIT

The main purpose of this program is to fit the Gaussian function to photopeak data with the least squares method. Calculations of the area under the Gaussian curve, resolution percentage of the peak, the non-linearity of the peak location corresponding to the photon energy, the saturated count rate, and specific count rate are all included in this program, and also the fitted Gaussian curve can be examined with the student-t and the χ^2-test based on the theory of statistics.

The computer program DIRFIT was written in FORTRAN IV language for use on the IBM 360/65 computer. The flow diagram is shown in Figure C-1.

The data input to DIRFIT are:

(1) name of isomer, its half-life, and energy of gamma-rays,

(2) datum number, mass of sample, waiting and counting times,

(3) calibrated units in keV/channel, and various indication numbers for calculations,

START

READ:
DATA INPUT

ACTUAL COUNT BY SUBTRACTING BKG

CONSTANT,B BY ITERATION

CONSTANT,x_o BY ITERATION

CONSTANT,A_{max} BY ITERATION

CONVERGENCE
CRITERION
=0.0001

AREA, RESOLUTION %, PEAK LOCATION

SATURATED COUNT RATE BY TIME CORRECTION

GAUSSIAN-FITTED VALUE FOR EACH CHANNEL

STUDENT-t; z-VALUE FOR EACH CHANNEL

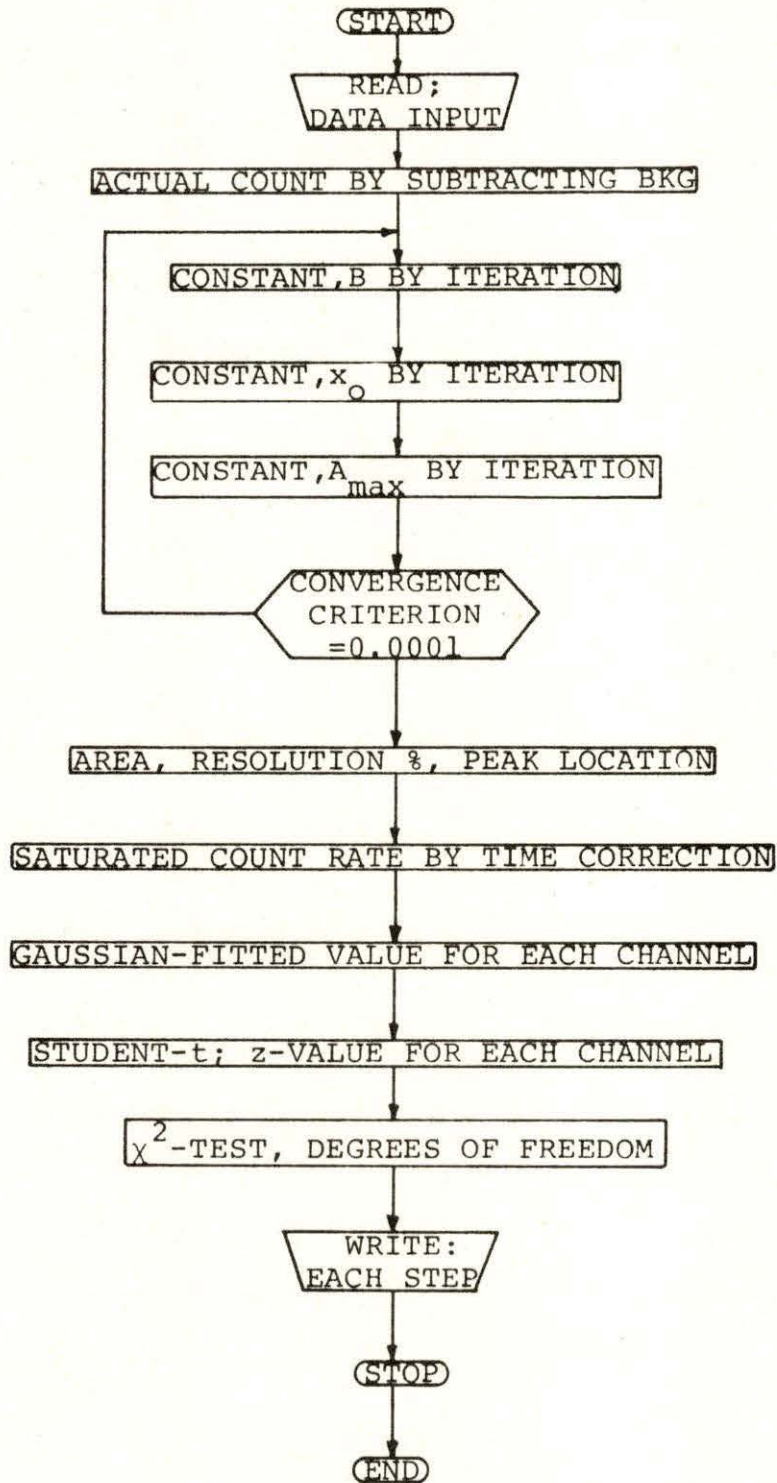χ^2-TEST, DEGREES OF FREEDOM

WRITE:
EACH STEP

STOP

END

Figure C-1.   Flow diagram of computer program, DIRFIT

(4)   initial values of the three constants of the
      Gauss function,

(5)   differences of those constants for large
      iteration,

(6)   steps of those constants for individual iteration,

(7)   data of source counts and background in 100
      channels around the photopeak.

A fitted curve and data points are illustrated in
Figure C-2. The fitted function is evaluated with DIRFIT,
and it is given by

$$G(x) = 1440 \exp[-0.00725(x-66.8)^2], \qquad (C-1)$$

where the channel at x=0 is No. 100 of full scale.

D.   Subroutine CURFIT

Bevington (32) discussed least-squares fit to an
arbitrary function with computer programs. He recommended
"CURFIT" as the fastest of the set discussed. It is mean-
ingful to use this program and to compare with the DIRFIT
program which was discussed in Appendix C. As mentioned in
the theory section of this thesis, the objective of the
CURFIT program is to find a Gaussian peak plus a quadratic
background function to fit photopeak data from a gamma
spectrum in the least squares sense. That function is
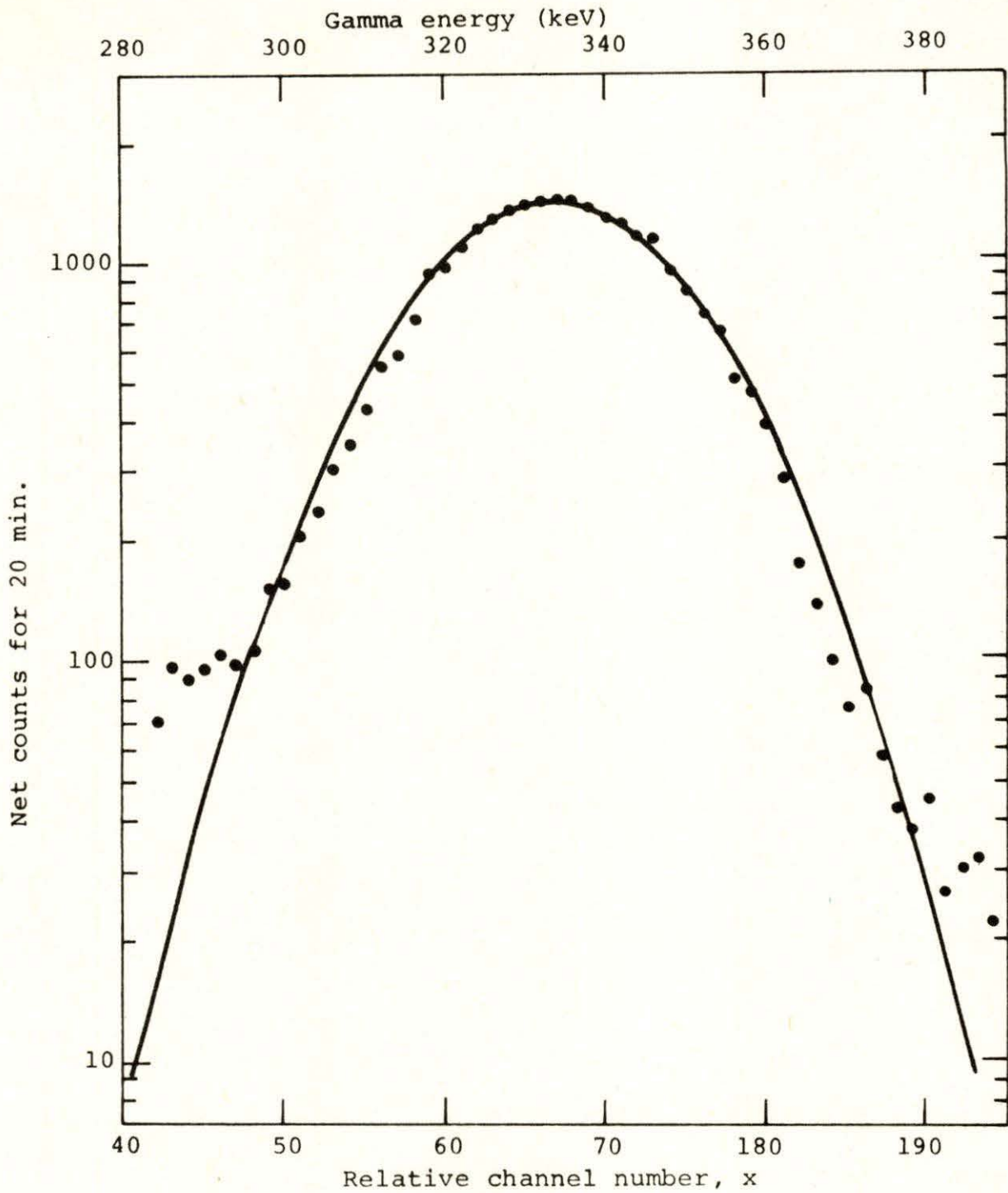written again,

Figure C-2. Photopeak and Gaussian fitting with DIRFIT program (The data correspond to No. 6 of indium (c.f., Table E-1))

$$y(x) = a_1 \exp\left[-\frac{1}{2}\left(\frac{x-a_2}{a_3}\right)^2\right] + a_4 + a_5 x + a_6 x^2 , \qquad (D-1)$$

where a_j (j=1,...,6) are constant parameters. From the output of the program, each parameter is printed out with its standard deviation.

The subroutine CURFIT consists of two subroutines and two function subprograms. The names of the subroutines and their functions are briefly discussed:

Subroutine CURFIT   This program is designed to make a least-squares fit to a function using the algorithm of Marquardt which combines a gradient search with an analytical solution developed from linearizing the fitting function.

Function FUNCTN   This program evaluates terms of the function for non-linear least-squares search with the form of a Gaussian peak plus quadratic polynomial of Equation D-1.

Function FCHISQ   This function subprogram evaluates reduced χ^2 for a set of data points y_i and a fitted function $y(x_i)$. The χ^2 is defined as

$$\chi^2 \equiv \Sigma\left\{\frac{1}{\sigma_i^2} [y_i - y(x_i)]^2\right\} . \qquad (D-2)$$

Subroutine FDERIV   This program evaluates the derivatives of the Gaussian plus quadratic polynomial function of Equation D-1. The user supplies analytical expressions

for the derivatives Δ_j of the parameters a_j ($j=1,\ldots,6$).

Subroutine MATINV   The computation for matrix inversion is provided in this program. This is used to invert a square symmetric matrix and to calculate its determinant.

The CURFIT routine was used to fit a function to experimental data of indium (number 12), and the result is plotted in Figure D-1. If counts in channels around both tails of the photopeak are at the level of background, the polynomial curve could be a measure of background. If however, the Compton edge and photopeak in a gamma spectrum begin to merge and the valley between them is higher than the level of background, then the fitted polynomial function does not correspond to the background. Therefore, the area between the Gaussian plus polynomial curve and the polynomial curve is not the same as the area under the Gaussian curve which is fitted with the direct fitting method discussed in Appendix C. In this connection, the fitting functions for datum No. 12 of indium, which are evaluated by two methods (i.e., programs DIRFIT and CURFIT), are:

DIRFIT: $G(x) = 2619 \exp[-0.00834(x - 67.56)^2]$,   (D-3)

where $x = 0$ is channel No. 100.

Figure D-1. The Gaussian plus polynomial function fitted to photopeak data
(The data corresponds to No. 12 of indium)

$t_i \simeq$ 50 hours

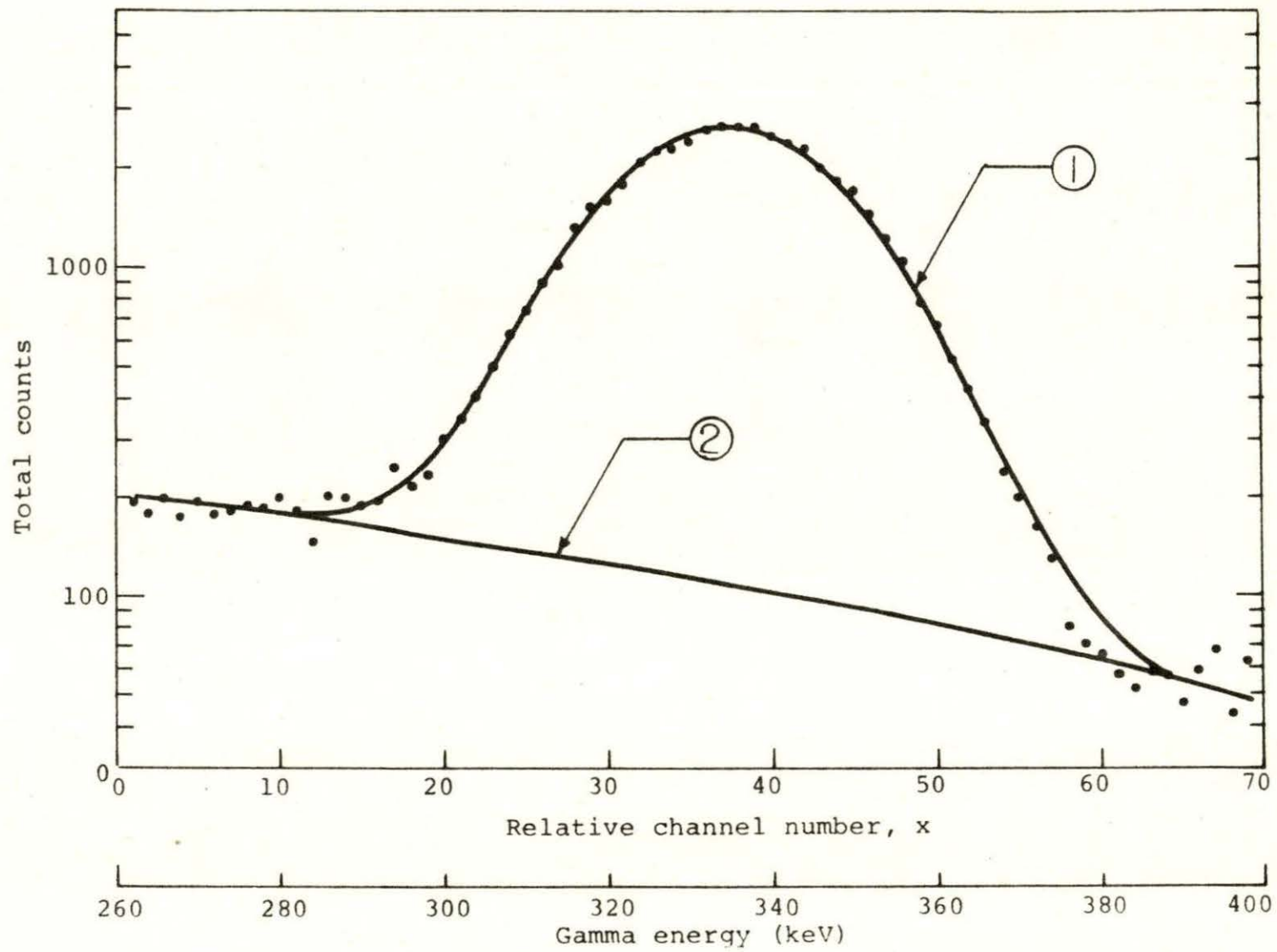t_w = 213 mins.

t_c = 20 mins.

Sample mass = 2223.6 mg

Curve 1. Gaussian plus second order polynomial

Curve 2. Polynomial only

$$\text{CURFIT:} \quad y(x) = (2556 \pm 15)\exp[-\frac{1}{2}\{\frac{x-(37.45+0.04)}{(7.31 \pm 0.05)}\}^2]$$

$$+ (205.1 \pm 5.3)-(2.9 \pm 0.56)x+(0.009 \pm 0.008)x^2,$$

$$(D-4)$$

where x=0 is channel No. 130. This function is illustrated in Figure D-1 with data points of the photopeak.

The computer time needed to fit photopeak data with the CURFIT is approximately one-fourth of that with DIRFIT.

E. Data Tables

In the following tables, all experimental data and calculated results are listed. Twelve samples of indium and seven samples of cadmium were examined. For the experimental results of datum numbers 2 and 4 of cadmium, calculations were tried twice for each result with different degrees of freedom, and those results are indicated as 2' and 4' for the datum number.

To simplify the information in the table, the following symbols are used, and their definitions are the same as those in the text:

No. = datum number,

W = mass of sample in mg,

t_w = waiting time in minute,

t_c = counting time in minute,

$C_T \pm \sigma_T$ = total net count under modified photopeak with its standard deviation given by $\sigma_T = \sqrt{C_T}$ in counts,

$R \pm \sigma_R$ = count rate at the end of the irradiation defined by Equation 9 with its standard deviation in cpm,

$\mu_i \pm \sigma_i$ = specific count rate for each sample with its standard deviation, which is given by $\mu_i = R/W$ and $\sigma_i = \sigma_R/W$, in cpm/mg.

In Table E-2 and E-4, the values of "Non-linearity of Energy" are defined as energy fraction η and given by

$$\eta = 1 - \frac{(\text{peak location})(\text{calibration unit})}{E_\gamma}, \qquad (E-1)$$

where calibration unit is 2 keV/chan. and E_γ is 335 keV for In-115m and 247 keV for Cd-111m.

Table E-1. General data of indium activation analysis

No.	W	t_w	t_c	$C_T \pm \sigma_T$	$R \pm \sigma_R$	$\mu_i \pm \sigma_i$
1	118.2	6	20	5525+75	288+4	2.433+0.034
2	235.4	40	20	9710+99	551+6	2.340+0.026
3	356.5	185	20	11573+108	948+9	2.635+0.026
4	597.9	109	20	20290+143	1371+10	2.293+0.017
5	833.7	220	20	21871+148	1957+14	2.347+0.017
6	954.2	150	20	29968+174	2246+14	2.354+0.015
7	117.2	6	40	11005+105	294+3	2.506+0.026
8	245.5	71	20	10946+105	672+7	2.736+0.029
9	372.2	105	20	12991+114	869+8	2.334+0.022
10	484.7	142	20	15258+124	1121+10	2.312+0.021
11	1002.3	179	20	30307+175	2444+15	2.438+0.015
12	2223.6	213	20	51150+227	4495+20	2.022+0.010

Table E-2.   Photopeak and statistical test data of indium

No.	Mass (mg)	Peak height	Peak width	Resolution %	Peak location	Non-linear Energy	ν	χ^2
1	118.2	287.6	18.0	10.8	164.88	-0.0156	9	12.37
2	235.4	480.0	19.0	11.3	165.89	-0.0096	17	28.98
3	356.5	504.8	21.5	12.9	165.05	-0.0146	9	9.91
4	597.9	1034.0	18.4	11.0	166.60	-0.0054	9	9.57
5	833.7	1049.0	19.6	11.7	166.22	-0.0077	9	8.01
6	954.2	1440.0	19.6	11.7	166.78	-0.0043	9	2.77
7	117.2	549.3	18.8	11.2	165.30	-0.0131	9	9.97
8	245.5	507.1	20.3	12.1	167.44	-0.0004	9	4.82
9	372.2	658.5	18.5	11.1	167.29	-0.0013	9	5.16
10	484.7	788.7	18.2	10.9	167.07	-0.0026	9	7.08
11	1002.3	1401.0	20.3	12.1	167.38	-0.0007	9	4.52
12	2223.6	2627.0	18.3	10.9	167.68	+0.0011	9	15.67

Table E-3.   General data of cadmium activation analysis

No.	W	t_w	t_c	$C_T \pm \sigma_T$	$R \pm \sigma_R$	$\mu_i \pm \sigma_i$
1	258.3	2	20	1097±33	65±2	0.2512±0.0052
2	556.4	4	20	3172±57	193±4	0.3470+0.0072
2'				3306∓58	201∓4	0.3615∓0.0072
3	815.8	3	20	2339+49	164+4	0.2014+0.0050
4	1119.9	5	20	4315+66	266+5	0.2378+0.0045
4'				5082∓72	314∓5	0.2801∓0.0045
5	258.4	2	40	1603+41	54±1	0.2094+0.0078
6	779.0	2.5	40	5274+72	179±3	0.2302+0.0039
7	2234.0	4	40	14221±120	494+5	0.2211±0.0023

Table E-4. Photopeak and statistical test data of cadmium

No.	Mass (mg)	Peak height	Peak width	Resolution %	Peak location	Non-linear energy	ν	χ^2
1	258.3	82.8	12.45	10.08	123.86	+0.00290	10	13.39
2	556.4	156.7	19.02	15.40	123.17	-0.00268	10	9.73
2'		155.9	19.92	16.13	123.11	-0.00316	7	9.05
3	815.8	208.9	12.32	9.97	124.05	+0.00444	10	8.64
4	1119.9	272.3	14.88	12.05	123.70	+0.00161	10	17.96
4'		280.1	17.04	13.80	122.73	-0.00624	3	0.74
5	258.4	121.6	12.39	10.03	122.90	-0.00486	8	16.01
6	779.0	364.8	13.58	11.00	123.90	+0.00323	10	15.58
7	2234.0	966.0	13.83	11.20	125.03	+0.01238	10	12.07